UPPSALA
UNIVERSITET

Digital Comprehensive Summaries of Uppsala Dissertations from the Faculty of Science and Technology 225

Solution-Chemically Derived Spectrally Selective Solar Absorbers

With System Perspectives on Solar Heating

TOBIAS BOSTRÖM

ACTA
UNIVERSITATIS
UPSALIENSIS
UPPSALA
2006

ISSN 1651-6214
ISBN 91-554-6663-X
urn:nbn:se:uu:diva-7160

Dissertation presented at Uppsala University to be publicly examined in Polhemsalen, Ångströmlaboratoriet, Lägerhyddsvägen 1, Uppsala, Friday, October 20, 2006 at 10:00 for the degree of Doctor of Philosophy. The examination will be conducted in English.

Abstract
Boström, T. 2006. Solution-Chemically Derived Spectrally Selective Solar Absorbers. With System Perspectives on Solar Heating. Acta Universitatis Upsaliensis. *Digital Comprehensive Summaries of Uppsala Dissertations from the Faculty of Science and Technology* 225. 91 pp. Uppsala. ISBN 91-554-6663-X.

This thesis consists of two parts, one dominating part concerning spectrally selective solar absorbers and one dealing with thermal solar systems. The appended papers I to VIII concern the solar absorber part, papers dealing with the systems part have not been included in the thesis.

A new spectrally selective absorber derived from a novel solution-chemistry method has been developed and optimized. The main objective was to investigate the potential of the spectrally selective surface. Some of the questions at issue were; would it be possible to create a suitable absorber composite using this method, how high selectivity could be obtained, could the performance be enhanced by using anti-reflection coatings, which was the optimal layer composition, would the thin films be durable and what was the structure and morphology like on a nano scale? The absorber consists of absorbing thin films of nickel nano-particles embedded in a dielectric matrix of alumina and an overlying anti-reflection film consisting of one of the following materials silica, hybrid-silica, alumina or silica-titania. Solution and sol-gel chemistry were used in the process. The thin films were spin-coated onto an aluminum substrate followed by a heat-treatment that generated the multi layer selective solar absorber.

The optical constants for the thin film materials in question were determined. An optimal three layer structure was modeled using the experimentally determined optical constants. The theoretical three layer stack was experimentally confirmed and achieved a solar absorptance of 0.97 and a thermal emittance of 0.05 which definitely are commercially competitive values. The configuration of the three layer stack is: an 80%nickel-20%alumina film at the base, a 40%nickel-60%alumina film in the middle and a silica or hybrid-silica film at the top. The three layer absorber was subjected to high temperature and condensation accelerated ageing tests designed by IEA Task 27. The condensation test did not degrade the absorber whatsoever but the high temperature test did reveal some oxidation of the nickel particles. The oxidation occurs initially and then stops. A formed nickel-oxide layer hinders further oxidation. The level of oxidation is small and the absorber is qualified according to the IEA Task 27 test procedure.

Keywords: solar, thermal, absorber, selective, chemical

Tobias Boström, Department of Engineering Sciences, Box 534, Uppsala University, SE-75121 Uppsala, Sweden

ISSN 1651-6214
ISBN 91-554-6663-X
urn:nbn:se:uu:diva-7160 (http://urn.kb.se/resolve?urn=urn:nbn:se:uu:diva-7160)

To all of you that mean so much to me,
what would I do without you?!

This thesis is based on work conducted within the interdisciplinary graduate school Energy Systems. The national Energy Systems Programme aims at creating competence in solving complex energy problems by combining technical and social sciences. The research programme analyses processes for the conversion, transmission and utilization of energy, combined together in order to fulfill specific needs.

The research groups that participate in the Energy Systems Programme are the Department of Engineering Sciences at Uppsala University, the Division of Energy Systems at Linköping Institute of Technology, the Department of Technology and Social Change at Linköping University, the Division of Heat and Power Technology at Chalmers University of Technology in Göteborg as well as the Division of Energy Processes at the Royal Institute of Technology in Stockholm.

www.liu.se/energi

List of papers

This thesis is based on the following papers, which are referred to in the text by their Roman numerals I-VIII. Reprints are made with permission from the publishers.

I **Solution-chemical derived nickel-alumina coatings for thermal solar absorbers**
T. Boström, E. Wäckelgård and G. Westin
Solar Energy, **74**, 2003, p. 497-503.

II **Anti-reflection coatings for solution-chemically derived nickel-alumina solar absorbers**
T. Boström, E. Wäckelgård and G. Westin
Solar Energy Materials and Solar Cells, **84**, 2004, p. 183-191.

III **Optimization of a solution-chemically derived solar absorbing spectrally selective surface**
T. Boström, G. Westin and E. Wäckelgård
Solar Energy Materials and Solar Cells, in press.

IV **Optical properties of solution-chemically derived thin film Ni-Al_2O_3 composites and Si, Al and Si-Ti oxides**
T. Boström and E. Wäckelgård
Journal of Physics: Condensed Matter, **18**, 2006, p. 7737-7750.

V **Characterizing a Ni-Al_2O_3/SiO_2 solar thermal selective absorber**
T. Boström, S. Valizadeh, J. Lu, J. Jensen, G. Westin and E. Wäckelgård
Thin Solid Films, 2006, submitted.

VI **ERDA of Ni-Al_2O_3/SiO_2 solar thermal selective absorbers**
T. Boström, J. Jensen, S. Valizadeh, G. Westin and E. Wäckelgård
In manuscript.

VII Durability tests of solution-chemically derived spectrally selective absorbers
T. Boström, G. Westin and E. Wäckelgård
Solar Energy Materials and Solar Cells, **89**, 2005, P. 197-207

VIII Accelerated ageing tests of optimized solution-chemically derived selective solar thermal absorbers
T. Boström, J. Jensen, G. Westin and E. Wäckelgård
Proceedings of Eurosun 2006, Glasgow, Scotland.

Comments on my contribution
I am responsible for the major part of the writing in all publications and prepared all samples, performed all experiments and measurements apart from the parts mentioned below:
The alumina precursor solution was prepared by Annika Pohl and Åsa Ekstrand; SEM and TEM images were made by Jun Lu and Sima Valizadeh; ERDA measurements were made by Jens Jensen.

Publications not included in the thesis

IX Spectrally selective solar thermal absorber based on sol-gel and solution-chemistry methods
T. Boström, G. Westin and E. Wäckelgård
Proceedings of SOLGEL 2005, Los Angeles, USA

X Design of a thermal solar system with high solar fraction in an extremely well insulated house
T. Boström, E. Wäckelgård, B. Karlsson
Proceedings of ISES 2003, Göteborg, Sweden, 14 – 19 June, 2003.

XI Infrared Reflectance of direct current magnetron sputter deposited films of Ni93V7, Cu89Ni10Fe1(Mn) and Cu
K. Gelin, T. Boström, E. Wäckelgård
Thin Solid Films, **437**, 2003, p.25-33.

XII Thermal emittance of sputter deposited infrared reflectors in spectrally selective tandem solar absorbers
K. Gelin, T. Boström, E. Wäckelgård
Solar Energy, **77**, 2004, P.115-119

XIII Tvärvetenskaplig analys av lågenergihusen i Lindås Park, Göteborg
T. Boström, W. Glad, C. Isaksson, F. Karlsson, M-L. Persson, A. Werner
Program Energisystem, Arbetsnotat nr. 25, ISSN 1403-8307, 2003

XIV Sustainable Solar Housing, Volume 1: Strategies and solutions, Volume 2: Exemplary Buildings and Technologies from IEA Task 28
Editors, R. Hastings and M. Wall
James & James, ISBN 1-84407-326-1&2, to be published.

XV Energianvändning i bebyggelse – aktörer och teknik
T. Boström, K. Ellegård, W. Glad, A. Green, C. Isaksson, F. Karlsson, E. Löfström, M-L. Persson, P. Rohdin, A. Werner, E. Wäckelgård
To be published.

Cover photograph

Contents

Abbreviations

Latin symbols

$A(\lambda)$	*Absorptance*
Aux	*Auxiliary need*
b_0	*Incidence angle modifier coefficient*
d	*Thickness*
$e(\lambda)$	*Emittance*
E_g	*Band gap*
E	*Electric filed component*
f	*Fill factor*
F'	*Collector efficiency factor*
G	*Incoming radiation*
I	*Intensity*
I_p	*Intensity of black body radiation*
I_{sol}	*Intensity of solar radiation*
k	*Extinction coefficient*
$K_{\tau\alpha}$	*Incidence angle modifier*
L_T	*Storage tank losses*
$(mC)_e$	*Thermal inertia of the collector*
n	*Real part of the refractive index*
N	*Complex refractive index*
PC	*Performance criterion*
q_u	*Useful delivered energy output*
r	*Amplitude reflectance*
$R(\lambda)$	*Reflectance*
S_F	*Solar fraction*
S_U	*Useful solar contribution*
t	*Time*
T_{DHW}	*Domestic hot water set temperature*
T_s	*Final temperature*
$T(\lambda)$	*Transmittance*
ΔT	*Temperature difference*
U_{L1}	*First order heat loss coefficient*
U_{L2}	*Second order heat loss coefficient*

Greek symbols

α	*Absorption coefficient*
α_{sol}	*Normal solar absorptance*
ε_{Br}	*Effective dielectric function*
ε_{therm}	*Normal thermal emittance*
λ	*Wavelength*
η_0	*Optical collector efficiency*
υ_s	*Spin rate*
θ	*Incidence angle*
$(\tau\alpha)$	*Transmittance absorptance product*
ω	*Angular frequency*
δ	*Phase shift*
φ	*Incident/transmitted angle*

List of constants

c	*Speed of light in vacuum*
h	*Planck's constant*
π	*Pi*

List of acronyms

A	Alumina
AcacH	Acetylacetone
AR	Anti-reflection
CER	Cumulative Energy Requirement
DHW	Domestic hot water
ERDA	Elastic Recoil Detection Analysis
HS	Hybrid-silica
IEA	International Energy Agency
MTES	Methyltrietoxysilane
S	Silica
SEM	Scanning Electron Microscope
SMHI	Swedish Meteorological and Hydrological Institute
ST	Silica-titania
TEM	Transmission Electron Microscope
TEOS	Tetraethoxysilane
TBOT	Tetrabutylorthotitanate

1 Introduction

This is my story, why this thesis came to be: It began when I started to watch television at the age of about seven. There were many programs dealing with global warming, pollution, energy-related problems, scarcity of food and water etc. As a child I thought I could solve a lot of these problems by finding THE ultimate energy source. Imagine what good you could do if you have unlimited access to sustainable energy! At that time in the eighties fusion power seemed to be the answer and I consequently wanted to be a fusion scientist. But as time passed I became more and more interested in solar energy, which in fact stem from an enormous fusion reactor, it is just that it is banked some hundred million kilometers from us. Solar energy is a down to earth technology with a lot of potential and it intrigues me. It took some time but here I am now in 2006 with a new Ph.D. thesis about solar thermal energy which I hope will make some impact on the solar energy society.

Now to become serious. New means of providing useful energy have to be found, due to the fact that our common energy conversion methods based on coal and oil combustion and nuclear power are not environmentally sustainable. One environmentally friendly alternative is solar energy. The amount of energy that strikes Earth's surface in the form of solar radiation can cover our world's energy demand many times over. The problems so far have been to convert the radiation into a usable form of energy and to store this energy. Commercially available photovoltaic devices which convert radiation into electricity suffer from high costs and low conversion efficiency, but there is continuous progress in this area. Solar thermal systems that convert radiation into heat can compete today with for example, oil burners and electrically driven resistance heaters, but they are still quite expensive. Consequently it is important to reduce the manufacturing costs of solar technology and to increase the efficiency and acceptance of solar thermal systems.

The thesis is divided into two parts, one dealing with solar collector systems and one with solar collector components – the spectrally selective absorber. The first part relates to solar thermal systems; how to make them more efficient and cost effective. The system's work aims at adapting solar thermal systems to the new generation of well-insulated houses and to designing systems with higher solar fractions, so the cost per produced kWh can be reduced. The most extensive and second part concerns a novel method to

manufacture spectrally selective surfaces, which has the potential of lowering the cost of the solar thermal absorber and producing full plate absorbers which could be used in building integrated solar collectors.

The work presented in this thesis is part of the national graduate school Energy Systems Programme. The study has been carried out at the division of Solid State Physics, department of Engineering Sciences, The Ångström Laboratory, Uppsala University.

1.1 Solar thermal collector systems

A large portion of the energy used in the world is consumed within the building sector. In Sweden buildings utilize 39 percent [1] of the country's energy consumption. Energy is becoming more and more an expensive and treasured necessity, thus it would be of great value if the energy demand of a building could be decreased. The most obvious action is to increase the insulation level and thereby decrease the space heating demand. A new generation of houses, coming into production in Sweden from the year 2000, has almost twice the amount of insulation compared to standard buildings erected at the same time. Still, a well-insulated house has an all year round need for domestic hot water and a demand for space heating during the autumn, winter and spring which has to be covered, for example, by using solar thermal energy.

In order to utilize a thermal solar system to a larger extent at high latitudes the heat yield has to be boosted during spring and autumn and preferably also suppressed during the summer (to prevent overheating of the solar collector system). In short there are two ways of accomplishing this goal; either by increasing the tilt of the collector or by using concentrating systems. Alternatively a high all year round solar fraction can be obtained by long term storing of surplus heat from the summer period for usage during the winter period. The central aim of the work on solar thermal systems was to design thermal solar systems that can obtain a high solar fraction using both concentrating and non-concentrating systems, but not by utilizing long term storage.

Most of the work on solar thermal systems was done early in my graduate studies and is hence more thoroughly described in my licentiate thesis [2]. Publications dealing with systems such as a conference proceeding from ISES2003 [3], IEA Task 28 work [4] and Lindås Park [5] have not been included in this thesis but are summarized in chapter 2.

1.2 Selective surfaces

The most efficient thermal solar collectors for hot water production use a spectrally selective surface that absorbs and converts solar radiation into heat. There are already high-performing selective surfaces but there are several difficulties with some of them, such as long-term durability, moisture resistance, adhesion, scratch resistance and costly technically advanced production techniques. In order to make thermal solar collectors more accepted and widespread, the price per unit has to be reduced. The most costly component of a thermal solar collector is the spectrally selective surface. The cost has to decrease in order to make thermal solar devices more commercially interesting in Sweden where solar thermal energy still has a very low impact on the energy market. In contrast, it is mandatory to install a solar collector in new and renovated buildings in some southern European countries like Spain and Portugal or parts of countries, like Tuscany in Italy.

The first spectrally selective surfaces were developed using relatively simple electrochemical techniques. These processes can produce surfaces with excellent optical properties, but large amounts of chemicals had to be used and the chemicals involved were not environmentally friendly. The latest generation of spectrally selective surfaces is a more environmentally sustainable alternative. The production method is low in material consumption but the vacuum technique utilized is relatively complex.

The main aim of the thesis was to investigate the potential and adapt a newly invented solution-chemical method to produce a spectrally selective surface. Some of the questions at issue were; would it be possible to create a suitable absorber composite using this method, what level of selectivity could be obtained, could the performance be enhanced by using anti-reflection coatings, what was the optimal layer composition, would the thin films be durable and what was the structure and morphology like on a nano scale?

Advantages of the solution-chemical technique are that it is simple and easy to control, the coating can be manufactured under ambient pressure conditions, the chemicals involved are environmentally friendly and it is low in material consumption. The selective surface consists of solar absorbing thin films of nickel nano-particles embedded in aluminum oxide with an anti-reflection film of a dielectric oxide such as silica on top.

The thesis describes the research process involved from the first experimental trials of developing a single spectrally selective film using the solution-chemical method, to the later optimized three layer absorber. This new research area was hence first explored using only experimental methods. Later on, when I became more familiar with this new technique, a more refined

optimizing method including theoretical simulations was developed in order to achieve an optimal result. Materials characterization was important in order to validate the optical models in the theoretical simulations. The absorber was mainly characterized using reflectance measurements, Elastic Recoil Detection Analysis and Scanning and Transmission Electron Microscopy. Finally accelerated ageing tests of the absorbers were made in order to investigate the durability properties.

2 Solar thermal systems

It is really only in the last 30 years that solar energy systems have become commercially interesting. Before the 1970s there was only a small market for thermal solar appliances. Water heating, swimming pool heating and air conditioning were the few areas where thermal solar products were competitive [6]. After the oil crisis in the early 1970s, money and effort was put into research and development of thermal solar collectors systems, as well as photovoltaic conversion systems. A number of different systems were designed.

The gist of this thesis, chapters 3 to 12, deals with an important specific solar collector component, the selective surface. Even more important is how the complete solar collector system is designed and operated. If the system is put together or operated incorrectly a well designed system will easily malfunction or lose in performance. It is hence very important to have a broad systems view in order to obtain efficiently working technical systems in practice.

2.1 The socio-technical solar thermal system

Chapter 2 mainly deals with technical systems aspects but it is important to remember another part of a technical system such as a solar thermal collector, namely the user and its socio-technical impact on the system.

The people handling the technical system before the user acquires it are also very important. The retailer of a solar thermal collector is obliged to give the customer correct information and to sell an adequate system. The retailer should take into account the customer's conditions, for example, the collector location and hot water heat demand of the customer, which, for example, influence the size of the collector and storage tank. Furthermore, the installer of a solar collector has to take correct measures in order for the system to work optimally.

How a technical system is used can be very important for how well it works. The solar fraction for a solar thermal system can, for example, be affected by the user's hot water consumption profile. A higher solar fraction can be ob-

tained if the user concentrates the hot water consumption to the afternoon or evening when the storage tank is full of solar heated water. The usage of the auxiliary source can be reduced if the hot water consumption is concentrated to the evening instead of the morning.

It is important that the user get an easily understandable manual describing the technical system. A good understanding of, in this case, the solar thermal system makes it easier for the user to check if the system is working properly and if it is necessary to make adjustments so that the solar fraction and thereby the energy savings becomes as high as possible.

2.2 Solar thermal system components

The main components of a solar collector system are a solar thermal collector, a storage tank, a circulation pump, an auxiliary energy source and heat exchangers for the solar collector, the domestic hot water (DHW), loop and the space heating loop. A schematic picture of a DHW thermal solar system can be seen in Figure 2.6.

2.2.1 The collector

Three collector types, the flat-plate, the evacuated tube and the pool collector dominate the market today. The most common solar collector construction of these three is the flat-plate which can be viewed in Figure 2.1. The most important part is the absorber, which gains heat by using photo-thermal conversion. Absorbed heat is transferred to a liquid or gaseous medium which flows through a tube connected to the absorber. Heat can be lost due to convection, radiation and conduction. The convection losses are reduced by covering the absorbers with a transparent glazing and the conduction losses are decreased by insulating the collector box. Radiation losses can be reduced by manipulating the absorber surface, see chapter 3. The evacuated tube collector works in a similar way as the flat-plate but instead of having fiber glass insulation the absorber plate is surrounded by a vacuum. The evacuated tube collector has thus very small heat losses and higher efficiency than the flat-plate. In situ measurements have shown that evacuated tube collectors are about 50 % more efficient than flat-plates [7]. However, since vacuum techniques are costly, the evacuated tube collector becomes approximately twice as expensive as the flat-plate collector per absorber aperture area. Pool collectors are very simple and non-insulated and only work in the summer and then with lower temperatures than can be obtained with flat-plates or evacuated tubes.

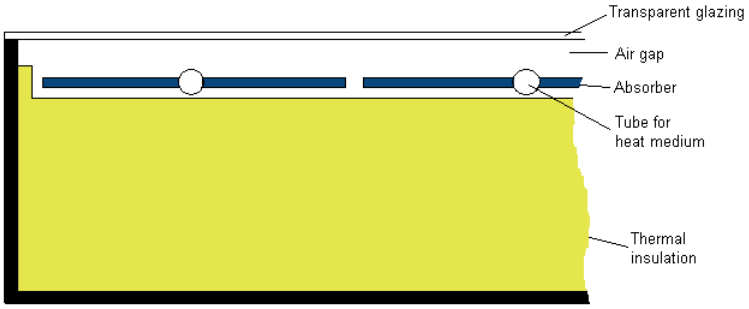

Figure 2.1. Schematic cross-section of a flat-plate solar collector.

Some facts about the three most common solar collector types are summarized below. Performance figures are calculated on a typical Stockholm climate. Cost figures are taken from the Swedish market in 2006.

- Flat-plate solar collectors have a maximum throughput of about 420 kWh/m^{2}a at an average temperature of 50°C. They cost from about 1 800 kr/m^2 and they cover about 90% of the Swedish market. Roof integrated flat-plate collectors can be seen in Figure 2.2a.
- Evacuated tube collectors have a maximum throughput of about 650 kWh/m^{2}a at an average temperature of 50°C and they cost from about 4 000 kr/m^2. Wall integrated evacuated tube collectors can be seen in Figure 2.2b.
- Pool collectors have a maximum throughput of about 450 kWh/m^{2}a at an average *temperature of 25°C* and they cost from about 900 kr/m^2. Pool collectors can be seen in Figure 2.3a.

A fourth type, the concentrating collector [8], utilizes an absorber fin, either free lying or inserted in an evacuated glass tube as the solar absorber. But the collector consists mainly of a highly reflective parabolically shaped non-focusing reflector that concentrates incoming solar radiation onto the absorber. There are two main reasons for using concentrating collectors. The collector becomes less expensive per area unit since the non-focusing reflector material, usually an aluminum foil, is less expensive than the selective absorber. Furthermore, it is possible to concentrate or reflect radiation incoming at selected solar height angles which makes it feasible to utilize the low standing northern sun to a higher extent and to avoid overheating problems during the summer. An example of a wall-mounted concentrating solar thermal collector can be seen in Figure 2.3b.

Figure 2.2. (a) Roof integrated flat-plate collectors in Gothenburg, Sweden. (b) Wall integrated evacuated tube collectors in Switzerland.

Figure 2.3. (a) Pool collectors in Malmö, Sweden. (b) Wall integrated concentrating collectors of MaReCo type in Aneby, Sweden.

2.3 Solar collector systems simulation models

Computer based simulation models of solar collectors are frequently used to derive the delivered energy output from the collector. Alterations in the collector are easily made and evaluated and compared to other simulated results or in situ measurements. Two different simulation tools were utilized, WINSUN which is a Swedish program developed by Bengt Peres and Polysun which is a commercially sold Swiss program.

2.3.1 Collector describing equations

The instantaneous optical and thermal response of a solar thermal collector is described by the law of energy conservation where q_u is the useful power per unit area of collector aperture, see equation 2.1 [9].

$$q_u = \bar{F}'(\tau\alpha)K_b(\theta)G_b + \bar{F}'(\tau\alpha)K_d(\theta)G_d - \bar{F}'U_{L1}\Delta T - \bar{F}'U_{L2}(\Delta T)^2 - (mC)_e\frac{dT_f}{dt}$$ Equation 2.1

The subscripts *b* and *d* stands for beam and diffuse radiation and *G* is the incoming radiation. The collector mean efficiency factor $\bar{F}'$ depends on the efficiency of the absorber to transfer heat from the fin to the fluid in the riser tube. The transmittance absorptance product *(τα)* takes into account the transmittance of the glazing, the absorptance of the absorber plate and multiple reflections between the absorber plate and the glazing [10]. The product of $\bar{F}'$ and *(τα)* is also known as the zero loss efficiency, η_0, and expresses the optical efficiency of the collector when operating at ambient temperature. U_{L1} and U_{L2} are the first and second order heat loss coefficients and the term $(mC)_e$ describes the thermal inertia of the collector. The temperature difference between the mean fluid temperature and the ambient temperature is denoted ΔT. The beam incidence angle modifier K_b is modeled with the standard equation 2.2 where b_0 is a collector-specific incidence angle modifier coefficient and θ is the incidence angle [10].

$$K_b = 1 - b_0\left(\frac{1}{\cos\theta} - 1\right)$$ Equation 2.2

The diffuse incidence angle modifier K_d is based on equation 2.2 but integrated over all angles [10].

2.3.2 WINSUN

WINSUN [11] is an abbreviation of a Windows version of MINSUN [12]. WINSUN and MINSUN can be used to obtain a calculated energy output from solar collectors. WINSUN is just as simple to use as MINSUN, the DOS version, but based and developed completely in PRESIM, TRNSYS and TRNSED Windows environments. Both programs use a dynamic collector model [13] which is based on the equations described in equation 2.1-2.2. But in WINSUN the operating temperature for the collector is determined for each time step in a full TRNSYS system simulation including piping, loops, tank, hot water and space heating loads. The storage component with stratification possibilities used in WINSUN is simulated in three layers.

Only a limited set of first order input variables are left open to the user to vary. The program utilizes climate data including ambient temperature and diffuse and beam radiation to achieve an accurate estimation of the energy output. A weather data file of a typical year was assembled from data col-

lected by SMHI (Swedish Meteorological and Hydrological Institute) in Stockholm during 1983 - 1992.

2.3.3 Polysun

In the Swiss simulation program Polysun the operator can vary close to a hundred different parameters. A special version of the program, the "Larsen editions" has been utilized which can read a heat demand output file from the building simulation program Derob-LTH [14]. The whole building can thus be simulated as accurately as possible by having the interface coupling between the two programs.

The collector describing model in Polysun is also based on the equations in section 2.3.1. The storage component with stratification possibilities used in Polysun is simulated in twelve layers. The used weather data file for the Stockholm climate was generated by Meteonorm [15].

2.3.4 Comparison between WINSUN and Polysun

A simulated case does not of course represent reality to a hundred percent, but today's simulation programs are good, at least if the simulated system can be physically defined and is robust. Large systems such as a climate model do still suffer from a large margin of error due to their inherent complexity. Solar thermal systems are, however, quite well defined and not very intricate. Still, it is hard to completely quantify a thermal solar system in a mathematical model and consequently the result from different numerical models will vary. Polysun, which has a more elaborate numerical algorithm compared to WINSUN allows the user to vary close to a hundred parameters. WINSUN can only vary about twenty parameters in total which makes it more simplified and not as detailed but on the other hand easier to use. It is important to use the models within their validated boundary limits.

A comparison was made by running as similar as possible simulations with the two simulation programs. Flat-plate solar combi systems were used and the load was defined according to section 2.6. The collector area was varied between 5 and 15 m^2 and the tilt angle was either 40 or 90º. *Fixed parameters* for both programs and each simulation were: a tank size of 1 m^3, Stockholm climate, the hot and cold water set temperatures, insulation levels of tank and piping, start and stop temperature differences for the pump, collector defining parameters and the load.

One difference between the two programs was the weather data. WINSUN used a typical year for Stockholm as data while Polysun had Meteonorm generated Stockholm weather data. The yearly solar irradiation on a horizon-

tal surface per m^2 in the WINSUN file was 921 kWh whereas the file in Polysun stated 981 kWh/m^2a.

The biggest difference between the programs seemed to be how they simulated the storage tank and the resulting tank losses. Polysun calculated a yearly storage loss of 615 kWh when the program was run with no collector; the corresponding value for WINSUN was 953 kWh. As the collector area was increased and hence the heat input to the tank, the storage losses should increase. Both programs show an increase in storage losses but the slope of the curves for Polysun was much steeper than for WINSUN, see Figure 2.4.

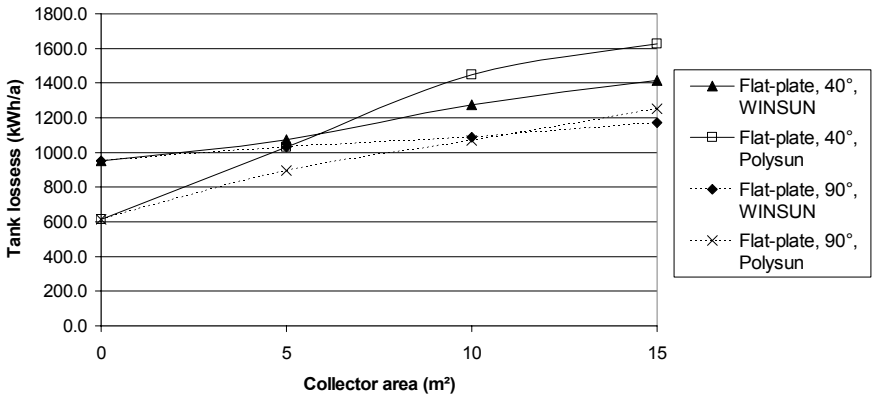

Figure 2.4. The tank loss dependence on the collector area and tilt angle in kWh per year.

Consequently since the storage losses were calculated differently, the annually remaining auxiliary demand also differed between the programs. This is the main reason why the curves for the two programs in Figure 2.5 do not begin at the same point and why they stay separated. It is also interesting to note that the 90º tilt is more favored in Polysun than in WINSUN, which is confusing since the solar collector output dependence on the tilt angle can be described by some straightforward equations. Furthermore, the remaining auxiliary demand was always lower in the Polysun model system even though the storage losses were higher (for large areas), see Figure 2.4. The remaining auxiliary demand from Polysun was generally about 10 % lower for collectors tilted 40º and about 16 % lower for collectors tilted 90º. The annual solar irradiation was 6.5 % higher for the data used in Polysun.

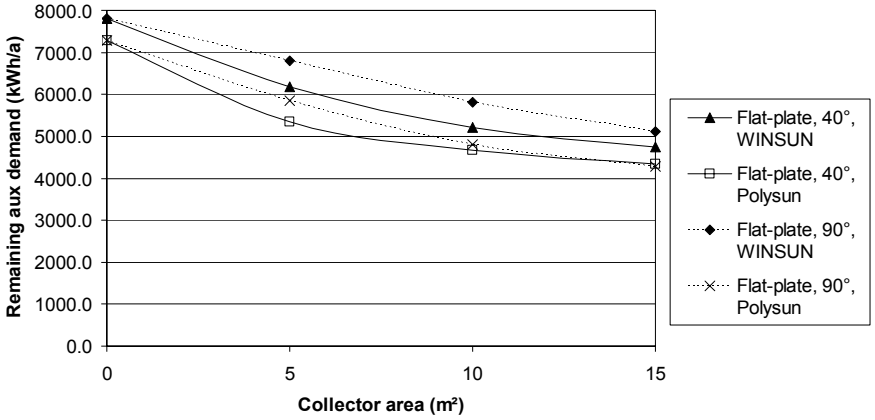

Figure 2.5. Remaining auxiliary demand as a function of collector area and tilt angle in kWh per year.

2.3.4.1 Discussion

The comparison between the two thermal solar collector systems simulation programs reveals some differences, especially concerning the tank calculations. The difference in tank losses between the two programs can partly be due to the fact that Polysun divides the tank into twelve layers while WINSUN only uses three layers. Consequently the stratification and heat losses will be calculated differently. A well stratified tank divided in twelve layers would perform more efficiently than the same tank divided into only three layers. Polysun calculates an about 5 % larger solar fraction compared to WINSUN when compensating for the difference in solar radiation between the used weather data. Consequently, the calculated solar collector output from Polysun is generally higher than for WINSUN.

2.4 Collector system studies

Non-concentrating roof mounted flat-plate or evacuated tube collectors (in the following text referred to as conventional collectors) have peak heat production during the summer. There is a rise in newly built houses in Sweden that are insulated to the extent that there is no heat load between April to October making the mismatch between solar yield and heat demand even worse.

In order to increase the solar collector efficiency during spring and autumn the system has to be altered. Theoretically a solar fraction of 100 % can be achieved by having large enough storage and a large collector area, but this concept can at present (2006) not be economically justified. However, An-

neberg, a newly built residential area outside Stockholm in Sweden, has a long term bore-hole rock storage for excess heat designed to give a solar fraction of 70% [16]. The surplus production of solar collectors in the summer is stored and pumped up in winter. Long-term storage is not dealt with in this thesis. Instead another alternative, using concentrating or wall mounted collectors which suppress the high standing summer sun and boost the low standing spring and autumn sun, has been studied.

It is complicated, costly and time consuming to make an in situ study on how a system reacts to changes of various system parameters. Simulation tools have therefore been used in order to be able to compare, for example, various collector types and the tilt angle effect easily. The two solar thermal collector system models Polysun and WINSUN were used in the studies.

Three different studies were made, one of an already built low energy housing project in Lindås Park, Gothenburg, one in the context of the International Energy Agency, IEA's Task 28, 'Sustainable Solar Housing' and one of high solar fractions using concentrating collectors. The parameter sets and variations in all three studies were within the limits for which the simulation programs have been validated.

2.5 Lindås Park

Twenty extremely well insulated terraced houses in Lindås Park, south of Gothenburg, were built in early 2001 [5]. The most distinct features of these houses compared to conventional terraced houses are the insulation level, the air tightness and as a consequence the absence of a conventional heating system. The living area is 120 m^2 divided into three bedrooms, a lounge, a kitchen, two hallways, two bathrooms and an attic. The walls have 40 cm of insulation compared to 20 cm which is the standard insulation thickness at present. The houses keep an indoor temperature of 20°C through a combination of an effective ventilation heat recovery exchanger and internal gains from body heat, solar radiation and appliances. Only if the outside temperature drops well below freezing point is there a need for extra heat. For these rare occasions an electric resistance heater of 900W is connected to the ventilation heat exchanger, which preheats the incoming air. A separate conventional DHW solar system designed to cover 50 % of the DHW load was installed for each house, since the terraced houses only have a DHW load and no space heating system.

The thermal solar system in Lindås Park was evaluated regarding the solar fraction and performance. Four out of 20 terraced houses have been monitored closely. The number of people occupying the houses varied from 1 to

4. The people living in the houses have been interviewed about their opinion on the installed thermal solar system. Did they think that it worked well or badly and was it easy to handle and maintain or not (user friendly)?

The installed system in each house was manufactured by Effecta-pannan AB and consists of a 5 m^2 flat plate collector with a selective absorber. The collector modules are integrated in the roof, which has an inclination of 27 degrees. The heat storage consists of a storage tank of 500 liters with two internal heat exchangers and an auxiliary electric immersion heater. A schematic picture can be seen in Figure 2.6.

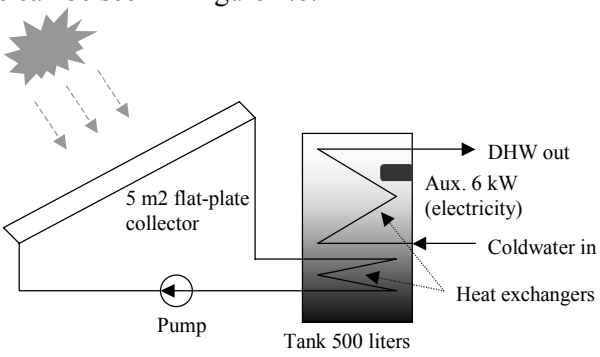

Figure 2.6. A schematic picture of the solar thermal DHW system installed in Lindås Park, Gothenburg.

2.5.1 Results

A detailed study of the Lindås Park solar collector system can be found in a comprehensive interdisciplinary study, although in Swedish [5].

The four terraced houses were monitored thoroughly by the Swedish National Testing and Research Institute. Hourly measured data of the DHW and the auxiliary electric immersion heater's energy consumption were used to calculate the solar fraction of the solar collector system. Tank losses, L_T, were estimated according to equation 2.3 for the two months December and January when the solar contribution is close to zero. The consumed energy for the domestic hot water and auxiliary source is noted E_{DHW} and E_{Aux} respectively. All through the remaining months, tank losses are assumed to be the same as the average value for December and January. The useful solar contribution S_U and the solar fraction S_F were calculated according to equations 2.4 and 2.5.

$$L_T = E_{Aux} - E_{DHW} \quad \text{(during Dec-Jan)} \qquad \text{Equation 2.3}$$

$$S_U = E_{DHW} + L_T - E_{Aux} \qquad \text{Equation 2.4}$$

$$S_F = \frac{S_U}{E_{DHW} + L_T}$$ Equation 2.5

DHW use, tank losses in winter time, auxiliary electric use for DHW and useful solar contribution in kWh/a can be viewed in Figure 2.7.

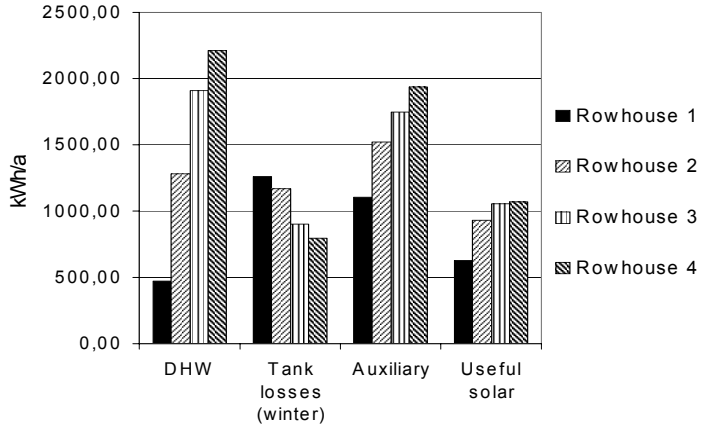

Figure 2.7. DHW use, tank losses, auxiliary electric use and useful solar contribution during one year for four row houses.

The study showed that the solar collectors did not perform as well as anticipated. The annual solar fraction, according to equation 2.5, was on average 37 %, compared with the design value of 50 %.

2.5.2 Conclusions

The major reason why a solar fraction of 50% was not obtained was most likely due to the thermostat temperature being set too high in the storage tank. In all cases it was set at more than 70°C and sometimes even above 80°C. A solar collector is most efficient when it operates at a low temperature, which was not the case here. Having this high set temperature also generated high storage losses, see Figure 2.7. A higher solar fraction would have been obtained if the temperature had been set at 55°C instead. The main responsibility for setting the correct temperature was on the installer, but also on the supplier of the solar collectors. This mistake could have been discovered by the occupants if they had had access to a well-written user's manual. Unfortunately that was not the case.

These are mistakes that should not have happened. However, what can be done is to learn from these mistakes and make sure that they are not repeated.

2.6 IEA Task 28

Task 28 “Sustainable solar housing” was a project (2001-2005) organized by the Solar Cooling and Heating group within the International Energy Agency, IEA. The purpose of Task 28 was to design cost effective buildings with a very low primary energy demand by reducing the energy losses and at the same time utilizing free energy, such as thermal solar energy. These aims can be achieved by having a well insulated climate shell, various combinations of passive and active solar radiation usage for heating and domestic hot water, high performance technical systems, sun screening and the use of natural day-lighting. The consumption of fossil fuels should be minimized. Three building types were studied in this project; single family houses, terraced houses and apartments. Suitable solution sets were developed for each type of building and for three different climate regions; cold (Stockholm), moderate (Zurich) and mild (Milan).

In order to get a fair comparison between different categories of energy supply Task 28 uses the notion Cumulative Energy Requirement. CER is a measure for the total amount of primary energy needed to deliver a product or a service. Primary energy resources include fossil and nuclear energy carriers (non-renewable), renewable energy (biomass, geothermal, hydro, solar, wind), but not waste products which are secondary resources. The sum of all primary energy sources needed to deliver a product or a service is the CER. Every energy source has a certain primary energy factor attached to it. The value of this factor depends on the impact that the energy source has on the environment. For example fossil fuels get high values while the factor for solar energy is close to zero.

Houses in Sweden built from the year 2000 and onwards usually have a CER of 100-150 kWh per m^2 living area and year, counting the energy needed for heating, DHW and household electricity. The goal of Task 28 is to design buildings that use less primary energy than 60 kWh per m^2 and year, excluding house-hold electricity needs. The space heating demand of the house (in order to keep an indoor temperature of 20ºC) was set at 25 kWh/m^2a or 3750 kWh/a. A typical single family detached house in the model is occupied by two adults and two children. The average DHW consumption in the model single family house is 45 liters per person and day [17]. Consequently, the model single family house consumes 180 liters of domestic hot water per day. The temperature of the hot water was set to 50°C, at the faucet. The on/off temperature set points for the thermostat in the tank were set to 55/57°C. The average inlet temperature, over the year, of the cold water in Stockholm is 8.5°C. With these parameters fixed, the resulting total DHW demand equals 3150 kWh/a or 21 kWh/m^2a.

2.6.1 Set up

The solar collector system simulation program Polysun was used to make a parametric study in this project. In the following section the sensitivity of the solar collector system towards a few key *optimization* parameters is shown, parameters such as the absorber area, the tank volume, the collector type and location (roof or wall), the hot water set temperature and system type (DHW or combi).

Rather than presenting the solar thermal collector system's energy conversion efficiency or solar fraction, the figures below show the remaining *auxiliary demand* per living area needed to cover the DHW and space heating requirements.

2.6.2 Results and discussion

The IEA simulation work is a pending publication [4]. A parameter study was made of a solar thermal collector system for the 150m^2 single family reference family house in a Stockholm type climate. The parameter study for the Task 28 work was based on common commercially existing technologies and hence concentrating solar collectors were not included.

2.6.2.1 Storage tank size

In short, the utilization of the solar gains from the solar collector increases with the size of the tank, but on the other hand the total heat losses also become larger. According to the simulations, the tank size does not play a central role. An optimum can be found at 0.6 m^3 for a 7.5 m^2 flat-plate solar collector combi system tilted 40º. Below this threshold the solar gains cannot be fully utilized and above the heat loss increase exceeds the increase in solar gains. It is important to note that the tank size should not be less than 0.4 m^3 in order to be able to cover the DHW and space heating demands during cold days.

2.6.2.2 Area

Figure 2.8 shows how the remaining auxiliary demand for a flat plate solar combi system for the simulated house varies during the summer months for collector areas between 5 and 10 m^2. When designing a conventional solar thermal collector system one should try to obtain 100% coverage during June to August. In the figure below it can be seen that 5 m^2 is too small an area to get complete coverage during the summer months. If the size is increased to 10 m^2 the auxiliary demand becomes non-existing from May to August and it is likely that the solar system will exhibit overheating problems during the summer. In addition the extra useful energy output from the last 2.5 m^2 is very small. The first 5 m^2 have an output of 360 kWh per year

and m^2, the useful output from the next 2.5 m^2 up to 7.5 m^2, is 135 kWh/m^2a and the useful output from the last 2.5 m^2 up to 10 m^2 is only 75 kWh/ m^2a. The life-cycle cost of one square meter flat-plate solar collector is approximately 50 kWh/a [4], which again shows that the last 2.5 m^2 are quite unnecessary. Consequently a suitable size is around 7.5 m^2.

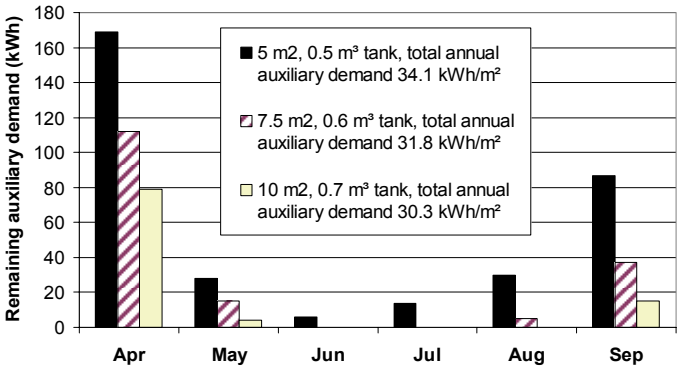

Figure 2.8. Dependence on collector area of the remaining auxiliary demand during the summer months for a solar combi system tilted 40º. The total annual auxiliary demand in kWh/m^2 (living area) is given in the text box.

2.6.2.3 Roof or wall collector

The Task 28 project was limited to only evaluating non-concentrating flat-plate and evacuated collectors. Table 2.1 shows how the annual auxiliary demand diminishes as the collector area is increased. Small systems tilted 40° are more effective than the vertical equivalent. However, having a 40 degree tilt generates a large amount of unusable heat during the summer for collector areas larger than 10 m^2. It is better to mount a large system vertically, as it then generates more in spring and autumn and avoids overproduction in summer. It is still not economically justified to double the collector area just to get a 12% decrease in auxiliary demand. Pros and cons of either location can be found in Table 2.2.

Table 2.1. Solar collector tilt effect on the remaining annually auxiliary demand in kWh per m^2 living area for a flat-plate solar combi system.

Collector area (m^2)	**7.5**	**10**	**12.5**	**15**
40° tilt	31	29	28	28
90° tilt	32	30	28	27

Additionally the simulations show that the efficiency of the collector will be more than 95 % of the maximum output as long as the azimuth direction is within +/- 30° from the south.

Table 2.2. Pros and cons of a roof or wall mounted non-concentrating flat-plate collector at a high latitude climate.

40º tilt		**90º tilt (vertical)**	
+	-	+	-
Can shut of the auxiliary system for a longer summer period	Susceptible to overheating during the summer	Acquires the highest solar fraction (large systems)	Needs larger areas
Small collector areas give a higher solar fraction	Becomes covered by snow in the winter	Easier to install	More easily shaded
Generally the more cost effective choice		Boosted solar radiation through snow reflections during the winter	Smaller available surface area to install the collectors on

2.6.2.4 Evacuated tube vs. flat-plate collector

Evacuated tube collectors have a higher efficiency compared to flat-plate collectors but are on the other hand about twice as expensive per square meter. To compare, the optimal flat-plate combi system of 7.5 m^2 tilted 40° which needs an auxiliary demand of 31 kWh/m^2a is matched with the vacuum system that needs the same amount of auxiliary energy. Resulting simulations show that 5 m^2 of evacuated collectors tilted 40° are sufficient to achieve the same efficiency. In other words the evacuated collector is about 50 % more effective per area unit than the flat-plate collector but since the evacuated collector is twice as expensive it does not become an economically justified choice. These findings correspond well with an in situ measurement [7] which showed that evacuated collectors were between 45-60 % more effective than flat-plates per m^2, depending on the load applied.

2.6.2.5 Hot water set temperature

A very important parameter, apart from the solar collectors and the storage tank, is the domestic hot water minimum set temperature, T_{DHW}, which is the actual temperature at the faucet. The temperature at the top of the tank is usually a few degrees higher in order to cope with the temperature drop from the tank to the faucet. T_{DHW} has been set to 50°C in the simulations above which is an adequate temperature for household purposes. Many solar collector systems have a much too high T_{DHW}, quite often up to 70°C or more, which results in the fact that the necessary auxiliary energy drastically increases, as in the case with Lindås Park, see section 2.5.2. Simulations show that the auxiliary energy demand for a 7.5 m^2 flat-plate combi system tilted 40°, increases by about 5% if T_{DHW} is increased from 50 to 60°C.

Legionella bacteria grow in still-standing water in the temperature interval 23-46°C and are killed above 60°C. Having a temperature in the tank of 50°C would hence be safe. In almost all modern tanks the tap water is heated using a heat exchanger, which minimizes the amount of still-standing water, thus effectively minimizing the risk of getting Legionella growth.

2.6.2.6 DHW vs. combi system

Both systems have 7.5 m^2 of flat-plate collectors tilted 40º and a 500 liter tank. The remaining auxiliary demand for the combi system was 31 kWh/m^2a (living area), the corresponding figure for the DHW system was 32 kWh/m^2a. Highly insulated buildings will consequently not benefit from having a conventional solar combi system; a DHW system will provide the same amount of useful heat since it is mainly the DHW load that is covered.

2.6.2.7 System losses

The system losses are dependent on several parameters and how the losses are actually defined. The losses provided by the solar collector simulation program are the tank losses, which include the total heat losses through the tank wall, base and cover and the connection losses. The tank losses become larger with an increase in tank size and/or increase of solar collector area. The annual tank losses for a solar system with 7.5 m^2 of collectors and a 600 liter tank are close to 1000 kWh per year or 7 kWh/m^2 (living area).

2.6.2.8 Primary energy use and CO_2 emissions

The emission of CO_2 equivalents for electricity is 430 g/kWh according to the EU_{17} mix of electricity in Europe. The CO_2 equivalent emission for biomass is 43 g/kWh and 247 g/kWh for natural gas. The primary energy conversion factor is 0.14 for biomass, 1.14 for natural gas and 2.35 for the EU_{17} mix of electricity. [18]

Two different cases were taken as examples; (1) a solar combi system with 7.5 m^2 collector area and an auxiliary biomass boiler and (2) a solar combi system with 7.5 m^2 collector area and an auxiliary condensing gas boiler. When using the factors above, the primary energy demand for the biomass case was 16 kWh/m^2a (living area) and the CO_2 emissions were 2 kg/m^2a (living area). The corresponding figures for the condensing gas boiler case were 45 kWh/m^2a and 9 kg/m^2a.

2.6.3 Conclusions

Evacuated collectors are not economically justifiable. The size of the tank is not crucial but the tank design is of great importance (insulation, connections, heat exchangers etc.) The collector area should be chosen in order to achieve 100% solar coverage during the summer months. The azimuth angle

is not crucial but should not deviate more than 30° from south. The collectors should preferably be placed on the roof, not the wall, unless one wants the highest possible solar fraction (not economical). Lowering the DHW set temperature to 50°C lowers the auxiliary demand. But one has to look into the legislation for each country and check what temperature levels are allowed. By using a stratifying heat exchanger unit instead of a coil, an approximately 0-10% lower auxiliary demand can be achieved. Lastly, but importantly, the benefits of a combi system are drastically reduced for highly insulated buildings.

2.7 Solar systems with a high annual solar fraction

The objective of this study was to examine how to increase the annual solar fraction of a solar thermal DHW system. The technique is to increase the output during spring and autumn while suppressing the output during the summer. Using concentrating systems with various acceptance angles is a very effective way of achieving this goal. The simulation program WINSUN has been used in order to estimate the output and surplus production for such solar collectors as flat-plate, vacuum and concentrating systems [3]. The solar fraction can be improved by increasing the collector area or by altering the solar collector system. In the following simulations a maximum surplus production of *50 kWh/month* was allowed, which is the boundary condition that determines the area of the collectors. The DHW load was set to 3150 kWh/a according to IEA Task28, see section 2.6. No space heating demand was applied in the model, just as in the case with the monitored houses in Lindås Park. Solar fractions were calculated according to equation 2.5.

2.7.1 Results and discussion

Figure 2.9 shows the solar fraction over the year for a flat-plate and an evacuated tube collector tilted 40 and 90º situated in Stockholm. A vertical collector can to a larger extent utilize the low standing winter sun and as seen from the figure the total solar fraction is increased from about 65 % to around 75 % if the tilt angle is increased from 40 to 90º. However, the collector area has to be approximately doubled.

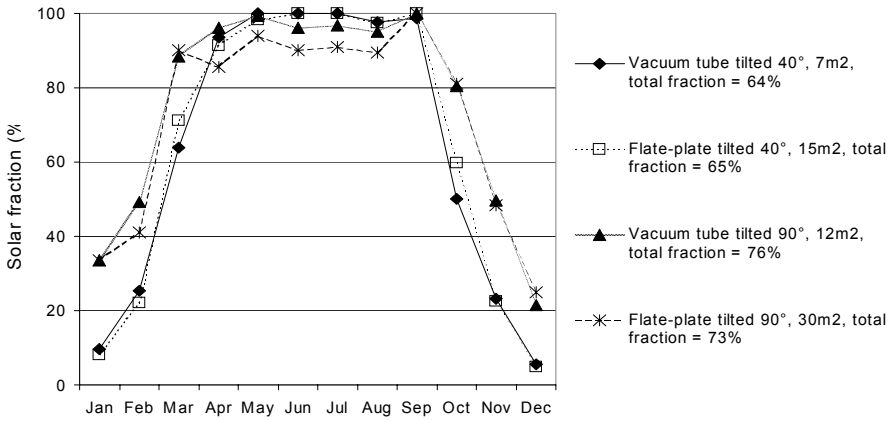

Figure 2.9. Glazed (absorber and concentrator) collector area, monthly and annual solar fraction for evacuated and flat-plate solar thermal collectors tilted 40° and 90°, allowing a surplus maximum production of 50 kWh/month.

The solar fraction can, as seen in Figure 2.10 be made much more constant over the year by utilizing concentrating collectors. The best result is achieved with the 12 m^2 wall mounted MaReCo [19] concentrating vacuum system which yields a high solar fraction from March to October and an annual solar fraction of 76%. The glazed area needed for this type of collector is 12 m^2 but the absorber area is only 4 m^2. The same solar fraction of 76 % was also, as seen in Figure 2.9, obtained with a non-concentrating evacuated tube collector mounted vertically, but this type required 12 m^2 of absorber area. To have the same coverage for a vertical non-concentrating flat plate system it needed to have around 30 m^2 absorber area.

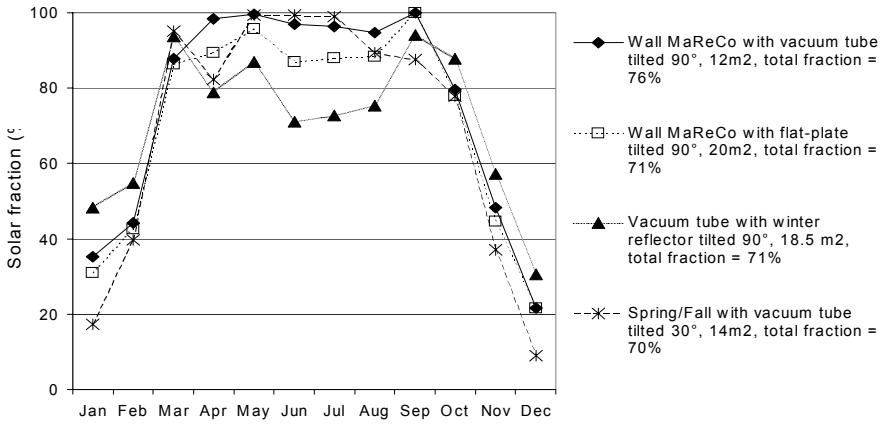

Figure 2.10. Glazed (absorber and concentrator) collector area, monthly and annual solar fraction for four concentrating solar thermal collectors, allowing a surplus maximum production of 50 kWh/month.

2.7.2 Conclusions

The solar fraction can be considerably improved by increasing the output during spring and autumn while suppressing the output during the summer. Simulations have shown that using concentrating systems with various acceptance angles is very effective in achieving this goal.

The highest annual solar fraction, 76%, with the smallest possible absorber area was obtained with a Wall MaReCo concentrating solar thermal collector using an evacuated tube as absorber. The glazed area needed for this type is 12 m^2 but the absorber area is only 4 m^2.

3 Solar thermal absorbers

Most absorbers are constructed as fin absorbers and consist of a metal plate that has good heat conductivity and high infrared reflectance such as aluminum or copper. The plate is coated with a thin surface layer that is spectrally selectively absorbing. The solar radiation is converted to heat in the surface layer and the absorbed heat is transmitted via the metal to a liquid or gaseous medium that is pumped through a pipe in contact with the metal, see also Figure 2.1. An ideal absorber surface should absorb all solar radiation but avoid losing the absorbed energy, i.e. heat, as infrared radiation. These properties are accounted for in a spectrally selective solar absorber.

There are other criteria for absorbers; they should easily conduct the produced heat to the heat transfer fluid in use, be long-term resistant to moisture and high temperatures and they should also be easy and inexpensive to produce. The most important reason why thermal solar collectors should be used to produce heat is that the energy conversion is accomplished in an environmentally sustainable way. In order to truthfully claim that a thermal solar collector is an environmentally friendly energy converting system the pollution impact of the materials used to produce it, the production and destruction chain have to be low.

Several different kinds of spectrally selective surfaces exist. Of these, four main types of absorbers can be distinguished in the literature [20-22]: intrinsic, tandem, textured surface and a heat-mirror type.

3.1 Solar and blackbody radiation

The optical design of an absorber surface is determined by the spectral distribution of solar and thermal radiation. Terrestrial solar radiation spectrally confined between 0.3 to 2.5 μm amounts for 98.5 % of the total incoming solar radiation. The maximum solar intensity is found at around 0.55 μm. The whole solar spectrum can be viewed in Figure 3.1, observe that the x-axis is logarithmic. When a surface becomes warmer than the surroundings it has a net radiation transfer to the surroundings. Thermal radiation is usually referred to as blackbody radiation, i.e. the maximal radiation to be emitted

for a certain temperature. The blackbody radiation distributions at the temperatures 100, 200 and 300°C are illustrated in Figure 3.1. The temperature of an absorber plate in operation is under normal conditions less than 100ºC.

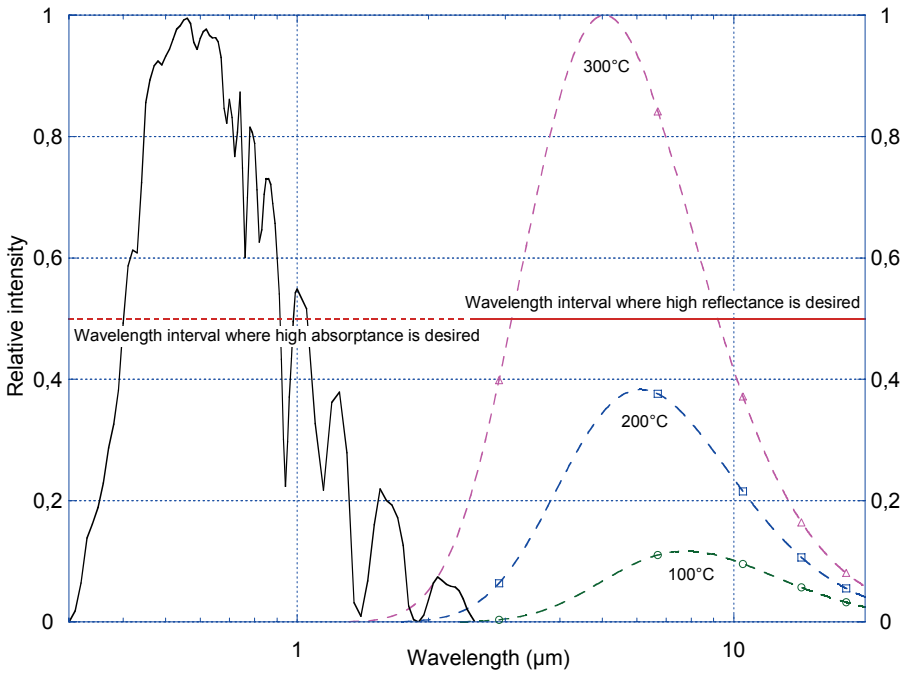

Figure 3.1. The solar irradiance distribution, solid curve (ISO standard 9845-1). Emitted radiation of blackbodies at 100, 200 and 300° C, dashed curves. The wavelength intervals where high absorptance and high reflectance of the absorber is desired are indicated in the figure.

3.2 Intrinsic absorbers

This is the most straightforward type of selective surface. It consists of a single substance with intrinsic optical properties that are wavelength selective. However, the transition from low to high reflectance either occurs at the wrong wavelength or is not sharp enough, and so far research on this type of material has not succeeded in creating a commercial product. The best absorber of this type, up to now, is made of ZrB_2 [23].

3.3 Textured surfaces

Special rough surface textures can be very efficient at trapping light, hence these types of coatings are also called optical trapping surfaces. The part of

the light that is not immediately absorbed in the surface is reflected deeper in between the surface dendrites and another portion is absorbed the next time it strikes the surface. These multiple reflections can lead to a high solar absorptance [21]. The long-wavelength emittance is practically unaffected by this texture.

3.4 Tandem absorbers

When researchers failed to obtain high solar selectivity in a single-phase bulk material, interest was focused on two layer structures. These tandem absorbers consist of two different surfaces, each with unique optical properties. Together they can exhibit a far greater spectral selectivity compared to what an intrinsic absorber could theoretically achieve. The easiest way of obtaining the desired optical properties is to create an absorber-reflector tandem. This type of absorber, which is also called a dark mirror, is made of a substrate with high infrared reflectance, i.e. low thermal emittance. Metals such as aluminum, copper, nickel, steel and silver fulfill this criterion. A thin film is added on top of the substrate. The film should be highly absorptive in the solar wavelength interval and highly transparent in the infrared wavelength interval. Commercially available high performing absorber-reflector tandems have been constructed using sputtered, electroplated, anodized or evaporated surface coatings on metal substrates, see also section 3.6. Several possible combinations of materials for constructing an absorber-reflector tandem are available.

3.4.1 Semiconductor/metal tandems

In order to create a high-quality solar absorber, all radiation with a wavelength shorter than 2.5 μm should be absorbed. This demand corresponds to a band gap, E_g, of 0.5 eV, according to equation 3.1.

$$\lambda \leq \frac{hc}{E_g} \qquad \text{Equation 3.1}$$

A semiconductor/metal tandem utilizes the fact that semiconductors exhibit material specific band gaps. Though some research has been done in this area, a commercially interesting product has still not been found. The largest obstacle to common semiconductors is that most of them have too large band gaps, corresponding to too short wavelengths. However, lead sulfide, PbS, is a suitable semiconductor with a band gap of 0.4 eV [21]. Unfortunately there is another indisputable problem with using PbS; the substance is very poi-

sonous, both for humans and for the environment. Unless a good way of recycling PbS can be found this material is not commercially feasible.

3.4.2 Multi – layer/metal tandems

An efficient spectrally selective solar absorbing surface can easily be tailored by using a multi-layer design. A multi-layer is constructed out of several alternate layers of semitransparent metal and dielectric materials. One example is an $Al_2O_3/Mo/Al_2O_3$ triple layer. Sputtering techniques are generally used to deposit this type of coating.

3.4.3 Thickness sensitive spectrally selective paint tandems

This tandem type of absorber utilizes inorganic pigments dispersed in a resin to capture solar radiation. It is an inexpensive [24] and simple way of creating a solar selective absorbing surface. Up to the present (2006) there is a significant disadvantage in using this kind of absorber; the normal thermal emittance value is very high compared to thin film metal – dielectric compounds.

3.4.4 Metal – dielectric composite/metal tandems

This absorber normally consists of metal or metal oxide nano-particles embedded in a dielectric matrix. A major advantage of this cermet is that it offers a high degree of flexibility. By varying the choice of particle, particle size, particle orientation and shape, film thickness and particle concentration in the film, innumerable combinations can be created. Thus solar selectivity can easily be tailored. Electroplating, sputtering, anodization, chemical vapor deposition and evaporation are some of the techniques previously used to produce these composite coatings.

3.4.4.1 Solution-chemically derived tandem

The investigated solution-chemical method produces an absorber that belongs to this group of tandem absorbers. The nano-particle material is nickel and the dielectric matrix consists of alumina. This is a well-proven and previously successful spectrally selectively absorbing composite that has been manufactured using various techniques. Craighead et al [25] produced nickel-alumina composites using coevaporation of metal and dielectric in the 70s. Andersson et al fabricated nickel pigmented alumina using electroplating in the 80s [26]. Sathiaraj et al [27] manufactured nickel-alumina composites using RF sputtering in the 90s.

The material choice, a nickel-alumina composite, was consequently a logical one when trying to produce spectrally selective absorbers using the new solution-chemical method.

3.5 Heat-mirror on black substrate

A heat-mirror on black substrate absorber makes use of the tandem idea but in an opposite way. The coating has to be highly reflective in the infrared wavelength interval and at the same time transparent to wavelengths in the solar spectrum i.e. a heat mirror. The substrate is selected to be a non-selective absorber with long-term durability properties. SnO_2:F on a substrate of black enamel is one of the previously investigated absorbers of this type [28].

3.6 Commercially produced absorbers

From Table 3.1 below it can be seen that absorbers with good selective optical properties already exist. However, there are a few difficulties when it comes to using some of the existing surfaces, for example, the long-term durability, the use of toxic substances in the production, complicated production techniques and cost. Costs have to be reduced to make thermal solar devices even more commercially interesting in for example Sweden, where solar thermal energy still has a very low impact on the energy market. The use of a solution-chemical method to create selective thin films has the potential of being an environmentally friendly and inexpensive way of manufacturing high performing selective solar absorbers.

Table 3.1. Performance comparison between some commercially available spectrally selective absorbers.

Company	Absorber/Substrate	Prod. method	α_{sol}^{*}	ε_{therm}^{*}
Sunstrip[29]	Ni-Ni_xO_x-CuNi /Aluminum	Sputtering	0.96±0.02	0.07±0.02
Alanod[30]	Cr_2O_3-$Cr(NO_3)_3$ /Copper	Sputtering	0.95±0.01	0.05±0.01
Helios [31]	Pigment /Stainless steel	Painting	0.91	0.25
MTI[32]	Black chrome /Copper	Electroplating	0.96±0.02	0.08±0.03
Tinox[33]	TiN_xO_x /Copper	Evaporation	0.95±0.02	0.05±0.02

*See section 4.2 for definitions

4 Optics of thin films

Constructing a well-designed spectrally selective absorbing surface requires understanding of basic electromagnetic wave theory. The section below describes how electromagnetic waves interact with matter in thin films.

4.1 Electromagnetic radiation and absorption

A plane electromagnetic wave propagating along the x-axis through an absorbing medium at time *t* is described by its electric field component, *E(x,t)* [34].

$$E = E_0 \exp(-k\omega x / c + i(n\omega x / c - \omega t)) \qquad \text{Equation 4.1}$$

E_0 is the initial amplitude of the electromagnetic wave of angular frequency ω before it enters the medium. The speed of light in vacuum is denoted *c*. The complex refractive index is given by equation 4.2.

$$N = n + ik \qquad \text{Equation 4.2}$$

The real part of the refractive index is denoted *n* which relates to the phase of the wave. The imaginary part is noted as *k* (also called the extinction coefficient) which describes a damping of the amplitude in the direction of propagation. The intensity is proportional to E^2 which leads to Beer's law which describes the change in intensity *I* of an electromagnetic wave when propagating through a medium.

$$I = I_0 \exp(-\alpha x) \qquad \text{Equation 4.3}$$

I_0 is the initial intensity before entering the medium and α represents the absorption coefficient. Combining equation 4.1 and 4.3, α is identified as:

$$\alpha = \frac{2\omega k}{c} \qquad \text{Equation 4.4}$$

The angular frequency ω can be expressed as equation 4.5 where λ is the wavelength of light in vacuum.

$$\omega = \frac{2\pi c}{\lambda} \qquad \text{Equation 4.5}$$

Assuming a thin slab *d*, equation 4.3 in combination with equation 4.4 and 4.5 results in equation 4.6

$$\ln\left(\frac{I}{I_0}\right) = -\alpha x = -\alpha d = -4\pi\frac{kd}{\lambda} \qquad \text{Equation 4.6}$$

which illustrates the relative intensity drop in a thin solar absorbing film. Equation 4.6, or more specifically the factor kd/λ, is of great importance when designing a spectrally selective surface. The film becomes transparent when $\lambda >> kd$. The transition from low to high absorptance at around 2 μm, according to Figure 3.1, is determined by the selection of *k* and *d*. An intrinsic type of absorber uses a single substance, which means that at a certain wavelength, *k* is non-changeable and *d* is the only variable parameter. An absorbing cermet offers more options. By altering the fill ratio or the size and shape of the metal particles, the *k* value of the cermet can be changed and subsequently the position of the transition step.

Equation 4.6 does not take into account thin film interference which can be used to improve the selectivity by making the transition step sharper.

4.2 Optical characterization of a selective solar absorber

Consider a ray of light impinging on a thin film. When the ray reaches the surface it is partly reflected at the front surface, absorbed in the film and/or transmitted through the film. The energy conservation in the interaction between the medium and the radiation is described by equation 4.7 where *A* is the spectral absorptance, *R* the reflectance and *T* the transmittance.

$$R(\lambda) + A(\lambda) + T(\lambda) = 1 \qquad \text{Equation 4.7}$$

Spectral emittance, *e*, is defined according to Kirchoff's law.

$$e(\lambda) = A(\lambda) \qquad \text{Equation 4.8}$$

The solar absorbing films that were made during this work were coated on an opaque aluminum substrate. Light transmitted through the film will partly be reflected back through the film and to a minor part be absorbed in the aluminum surface. The transmittance will therefore be equal to zero. Consequently, equations 4.7 and 4.8 can be rewritten as:

$$e(\lambda) = A(\lambda) = 1 - R(\lambda) \qquad \text{Equation 4.9}$$

Normal solar absorptance, α_{sol}, is theoretically defined as a weighted fraction between absorbed radiation and incoming solar radiation. The solar spectrum, I_{sol}, used here is defined according to the ISO standard 9845-1 (1992) with an air mass of 1.5.

$$\alpha_{sol} = \frac{\int_{0.3}^{4.1} I_{sol}(\lambda)(1 - R(\lambda))d\lambda}{\int_{0.3}^{4.1} I_{sol}(\lambda)d\lambda} \qquad \text{Equation 4.10}$$

Normal thermal emittance, ε_{therm}, is also a weighted fraction, but between emitted radiation and the Planck black body distribution, I_p, at 100°C.

$$\varepsilon_{therm} = \frac{\int_{2.5}^{20} I_p(\lambda)(1 - R(\lambda))d\lambda}{\int_{2.5}^{20} I_p(\lambda)d\lambda} \qquad \text{Equation 4.11}$$

Non-normal incidence measurements are also of interest, especially for the thermal emission which is completely diffuse in appearance. However, it is much more difficult and time consuming to measure non-normal incidence, so the solar energy society normally only present results based on normal incidence measurements. More about non-normal incidence and solar thermal absorbers can be found in [22].

4.3 Fresnel formalism

Equations describing the amplitude and intensity reflectance of a solar absorbing surface can be derived from the Fresnel formulas when applying them to a thin film case. [34]

For simplicity, consider a case of a single thin layer of thickness d and complex refractive index N_2. The thin film is surrounded be vacuum, hence N_1 and N_3 is equal to one. Light reaches the surface of the film at an angle of incidence φ_1 and a part of it r_1 is reflected at the same angle. The other part t_1 is transmitted through the layer at an angle of φ_2. The backside of the film will reflect a part of t_1 equal to $t_1 r_2$ and these multiple reflections will continue theoretically in infinity. The transmission and reflection relations are governed by the Fresnel coefficients. The total reflectance is achieved by summing the successive amplitude contributions, each one with its phase. The total amplitude reflectance r can accordingly be written as

$$r = \frac{r_1 + r_2 e^{-2i\delta}}{1 + r_1 r_2 e^{-2i\delta}} \qquad \text{Equation 4.12}$$

where δ is the phase shift which can be formulated using Snell's law of refraction and equation 4.5.

$$\delta = -\frac{2\pi}{\lambda} N_2 d \cos\varphi_2 \qquad \text{Equation 4.13}$$

The intensity reflectance R is equal to the complex square of equation 4.12.

$$R = rr^* = \frac{r_1^2 + 2r_1 r_2 \cos 2\delta + r_2^2}{1 + 2r_1 r_2 \cos 2\delta + r_1^2 r_2^2} \qquad \text{Equation 4.14}$$

The investigated solar absorber in this thesis consists of up to three layers. The fact is that no really new problems arise when calculating the optical properties of a multilayer stack. Each layer (two boundaries) in the stack is treated separately, using the derived equations 4.12 to 4.14, using matrix calculations. The whole operation can however quickly become enormous in terms of arithmetic calculations. [34]

4.4 Effective medium model

Transmittance and reflectance of electromagnetic radiation traveling through absorbing composite films can be modeled using various theories. When determining the refractive index, see section 6.2, the method partly makes use of an effective medium model.

The effective medium model requires that the particles in the composite medium are much smaller than the wavelength of the incoming light. Usually a particle radius of 10 nm or smaller is sufficient. If this is the case then the electric and magnetic fields are approximately constant over the particle at any time for radiation in the solar spectral wavelength range. It will therefore be possible to calculate an average effective dielectric function of the composite, using effective medium theory. The Bruggeman approximation [35] was used to calculate such an effective dielectric function, ε_{Br}.

$$f_A \frac{\varepsilon_A - \varepsilon_{Br}}{\varepsilon_A + 2\varepsilon_{Br}} + (1 - f_A) \frac{\varepsilon_B - \varepsilon_{Br}}{\varepsilon_B + 2\varepsilon_{Br}} = 0 \qquad \text{Equation 4.15}$$

Necessary inputs for solving equation 4.15 are the dielectric constants, ε_A and ε_B, and the fill factors, f_A and (1 - f_A), of material A and B i.e. the metal and the dielectric components. The model assumes the particles to be spherical in shape and randomly intermixed.

4.5 Absorber performance enhancing methods

A surface will always reflect light, which in this case is undesired. An anti reflection, AR, layer can be deposited on top of the absorber in order to suppress this reflection.

4.5.1 Anti reflection optics

By using Fresnel coefficients r_1 and r_2, see section 4.3, for thin films the refractive index for an AR coating that gives zero reflectance for a bulk material can be deduced [36]. An AR coating is the most effective when its refractive index is equal to the square root of the refractive index of the material it is deposited on, assuming a vacuum surrounding. This formula is, however, only valid for non-absorbing dielectric materials where the base is a dielectric bulk. As a result, an AR coated absorber will show an increase in normal solar absorptance and providing that the AR coating is sufficiently thin (<100 nm) it will not increase the thermal emittance.

Dielectric oxides such as silica or titania can normally provide suitable refractive indexes in order to function as AR thin films. Sol-gel derived amorphous silica and titania have a refractive index of 1.4 [37] and 2.0-2.2 [38, 39] respectively. Thus refractive indices in the visible between 1.4 and 2.2 can be obtained by mixing silica and titania.

4.5.2 Graded index

A graded index design can also be used to boost absorptance values. Thin film interference in the solar wavelength range is suppressed by a continuous grading of the optical refractive index. This method is most efficient when the solar absorbing film has its highest concentration of particles at the metal/cermet interface and no metal at the front surface of the coating.

5 Sample preparation

The absorber was produced out of one or two absorbing layers and one AR layer. Both smooth highly specularly reflecting aluminum and optically rough aluminum were used as substrates. The surface roughness rms (root mean square) value of the rough quality is 0.25 μm and the smooth quality 0.02 μm [40]. The aluminum substrates measured 55 x 55 mm, large enough to avoid edge effects and small enough to fit into the furnace. The substrates had to be cleaned before being coated, since the coating solution adheres poorly onto a contaminated aluminum surface. An organic solution containing nickel and aluminum ion complexes coated on the substrate and following heat treatment formed the absorbing layer(s). Various sol-gel solutions that after another heat treatment formed oxides like silica, alumina and titania were added as AR layer.

5.1 Aluminum substrates

5.1.1 Optically smooth aluminum

This type of aluminum is manufactured with a thick protecting layer of alumina that has to be removed before it is ready for use. In order to remove the alumina an etching solution made of one liter of distillated water, 35 grams of chromium (VI) oxide and 20 ml of 85% phosphoric acid was used. The aluminum substrates were placed in heated (80°C) etching solution for eight minutes. Then the substrates were carefully rinsed in hot water followed by a flush of distilled water and finally dried by blowing nitrogen on the surface. By following this procedure a clean and pure aluminum surface was acquired, see Figure 5.1a. The imperfections on the aluminum surface originate from defects in the manufacturing procedure of the aluminum sheet.

Transmission electron images however show that there is a very thin layer of about 10 nm on top of the aluminum surface, see *paper V*. This thin layer most probably consists of alumina which is immediately formed when an aluminum surface is exposed to air.

5.1.2 Optically rough aluminum

The rough aluminum quality only had the naturally formed alumina thin film on its surface. There are also other unwanted substances such as grease and oil on the surface, mainly originating from the rolling mill procedure. In this case another type of etching solution was used, made of one liter of distilled water and 125 ml of 85% phosphoric acid. These substrates were etched for 20 minutes at 50°C and thereafter rinsed in distilled water and dried by blowing nitrogen on the surface. The resulting surface can be viewed in Figure 5.1b at 20 times magnification. The scratches are rolling grooves originating from the rolling process.

Figure 5.1a and b were captured with a digital camera connected to a light microscope of the make Olympus type BX60.

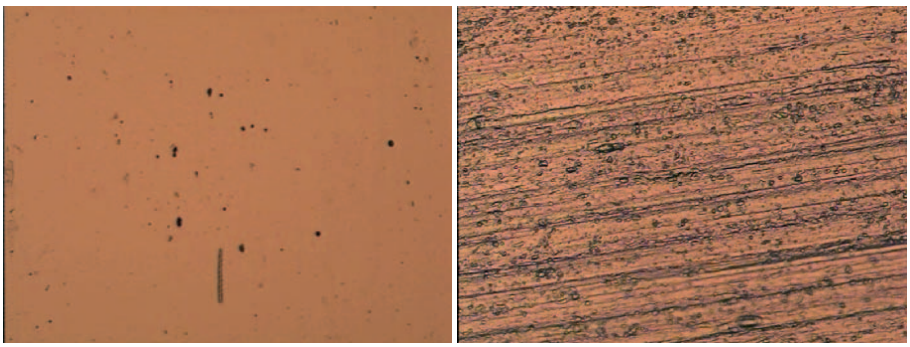

Figure 5.1a and b. Etched smooth and rough aluminum at 20 times magnification.

5.2 Absorbing layer solution

Sol-gel methods have been used to produce a wide variety of materials for many decades. But it is only in the last few years that solution-chemistry or sol-gel science was found to be a suitable method to produce nano-particles appropriate for thermal solar absorber applications. The solution-chemistry method investigated in this work was invented by Gunnar Westin, Uppsala University, and at present (2006) under a patenting process and can therefore not yet be described. However some basic information about the solutions can be found below. The chemicals used in this process are inexpensive and readily available.

5.2.1 Alumina precursor solution

An alumina solution was prepared. The concentration of aluminum ions in the alumina precursor solution was gravimetrically determined as amorphous

alumina; an exact amount of solution was dried in air and subsequently heated to 800°C in a platinum crucible to yield pure amorphous alumina. The formed alumina was accurately weighed and thus the Al ion concentration could be calculated.

The time until the alumina solution precipitated varied from 48 hours to two weeks. The most important parameter that determines the stability of the alumina solution seems to be the temperature. The stability of the alumina solution is substantially prolonged if refrigerated.

5.2.2 Nickel precursor solution

Nickel precursors were dissolved in solvents. The dissolution was complete and no gravimetric determination of the concentration was necessary. The nickel solution is long-term stable.

5.2.3 Nickel – alumina solution

Mixing precursor solutions of Ni and Al_2O_3 in different proportions controlled the nickel to alumina ratio of the absorbing films. The mixed alumina and nickel solution was stable for at least 24 hours. The stability could be increased up to one week if the solution was diluted with methanol.

5.3 Anti reflection oxide solutions

Five different amorphous oxide materials were studied, alumina, silica, hybrid-silica, and two compositions of silica-titania.

5.3.1 Alumina

The alumina solution is the same alumina precursor solution as was used for the absorbing base layer, see section 5.2.1.

5.3.2 Silica and hybrid-silica

The sol-gel route used to produce the silica and hybrid silica solutions originates from a paper by Tadanaga et al [41]. Tetraethoxysilane, TEOS, and methyltrietoxysilane, MTES, were used as starting materials. If only TEOS is used the resulting film will consist of 100% silica. Mixing TEOS and MTES will generate a hybrid silica solution, where the methyl group remains directly bounded to the silicon atom in the resulting hybrid film. The higher the proportion of MTES in relation to TEOS is the more flexible the resulting coating will be.

TEOS was mixed with ethanol before H_2O containing 0.06 wt% HCl was added to the solution. The resulting mixture was stirred for one hour at room temperature in order to hydrolyze TEOS. A proper molar ratio of MTES was then poured into the solution. After being stirred for 24 hours in a closed container, to ensure full hydrolysis, the obtained solution was used for coating. The molar ratios of ethanol and H_2O to the total alcoxide (TEOS + MTES) were 5 and 4, respectively. The mixed solution was stable for more than one week.

5.3.3 Silica-titania

The silica-titania mixtures were produced by using a sol-gel technique originating from Dawnay et al [42]. TEOS, ethanol, H_2O and HCl were mixed and stirred for 30 minutes. Ethanol was added to dilute the solution to a suitable concentration. Finally acetylacetone, AcacH, and tetrabutylorthotitanate, TBOT, were added and the resulting solution was stirred for 6 hours before being used. TBOT had to be added in drops in order to get a homogenous solution. The amounts of TEOS and TBOT were varied to get solutions with 70/30 and 50/50 Si/Ti molar ratios, respectively. The molar ratios of TEOS:EtOH:H_2O:HCl were 1:1:2:0.1 and TBOT to AcacH was 1:1. The mixed solution was stable for more than one week.

5.4 Coating process

There are several different ways of coating a surface with a liquid medium. Methods worth mentioning are spin-, flow-, spray- and dip-coating. The most suitable and used process for these laboratory experiments turned out to be spin-coating. Spin-coating methods utilize a spinner, where the number of revolutions per minute can be chosen. A spin coater of the make Chemat Technology and model KW-4A was used. A syringe with approximately 0.35 ml of coating solution was used to eject the liquid on top of the center of the substrate. In a fraction of a second the substrate was fully covered with coating solution and a completely homogenous and even film was acquired. Further evaporation of solvents and as a result an increase in coating stability was achieved by letting the spinning process continue for about 30 seconds after the solution was ejected.

By changing the spin rate, v_s, it it was possible to control the film thickness. Rates between 1200 to 6000 rpm were used. The total metal ion concentration of the solution is the second most important parameter that determines how thick the resulting film becomes. The higher the total metal ion concentration of the solution is, the thicker the film on the substrate becomes. The

metal concentration can be increased through evaporation of the solution solvents. Different surface structures and hydrophobic/hydrophilic properties of the substrate material can also influence the film thickness and/or film characteristics.

5.5 Heat treatment

After the substrate was coated it was heat treated inside a glass tube of 60 mm in diameter inserted in a split able furnace of type ESTF 50/14-S and make Entech. The environment had to be oxygen free in order to keep the formed nickel particles from forming nickel oxide.

Two parameters could be varied during the heat treatment process, the temperature increase rate and the final temperature, T_s. If the final temperature was set too low, residual organic groups would not be completely removed and a poor coating quality would be the result. The standard heat treatment for the absorbing layers was performed according to the following procedure; starting from room temperature the temperature was increased by varying speeds up to the final temperature at 550-580°C. The heat treatment for the AR layer varied in final temperature from 350 to 580°C but the temperature increase rate was always 50°min^{-1}. The samples were left in the furnace until the temperature had decreased to 300°C before they were removed and placed in room temperature to cool more quickly.

6 Methodology

The selected characterization methods were chosen in order to give physical and chemical knowledge about the solar selectively absorbing and anti-reflecting thin film materials. Reflectance measurements were carried out to be able to calculate the absorptance and emittance of the absorbers. Electron microscopy and atomic composition investigations were done in order to find out the nanostructure and morphology of the samples. When knowing the nanostructure it would also be possible to verify the optical absorber model described in section 6.2.

6.1 Characterization tools

6.1.1 Optical

The normal reflectance of prepared and aged samples was measured in the wavelength interval 0.3 to 20 μm. A Perkin-Elmer Lambda 900 spectrophotometer equipped with an integrating sphere of diameter 150 mm, circular beam entrance and sample ports of 19 and 25 mm, respectively was used in the wavelength interval 0.3 to 2.5 μm. The infrared wavelength interval, 2.5 to 20 μm, was measured with a Bomen Michelson 110 and a Bruker Tensor27 FTIR spectrophotometer; both set up with an integrating sphere of diameter 4 inches (102.4 mm) and a circular beam entrance and sample port of $1^{1/8}$ inches (28.8 mm). A sample of spectralon and an evaporated gold mirror was used as a reference mirror for the measurements done with the visible and the infrared spectrophotometer respectively. The measurements were combined to create one spectrum and the normal α_{sol} and ε_{therm} values were calculated using equations 4.10 and 4.11 [10].

6.1.2 Atomic composition

Heavy ion Elastic Recoil Detection Analysis (ERDA) is a well suited method used to measure the depth profiles of light and heavy elements simultaneously [43] and has previously been used to analyze atomic composition in solar selective absorbers [44]. Time-of-flight – energy ERDA (ToF-E ERDA) was used to measure the depth profile of the elements in the films

[43, 45]. A detailed description of the experimental set-up used has been given elsewhere [45]. The 5 MV tandem accelerator in the Tandem Laboratory at Uppsala University generates 45 MeV $^{127}I^{9+}$ ions that were used as projectiles in a forward elastic recoil configuration to produce target recoils. The ToF and energy signals for each recoiling ion were recorded, and the recoil energy spectrum was converted to elemental depth profiles [45].

6.1.3 Morphology

The film thickness and interface morphology was examined using transmission electron microscopy (TEM). The cross-sectional TEM thin slice specimens in *paper I* were prepared using the subsequent techniques cutting, drilling, dimpling and finally ion-milling [46]. The transmission electron microscope used to take the pictures in *paper I* was manufactured by JEOL, type JEM-2000FX II. Cross-sectional TEM specimens in *paper V* were prepared using a FEI Strata DB 235 dual-beam focused ion beam and scanning electron microscope (FIB/SEM) system. The FIB system is equipped with electron beam assisted deposition (EBAD) as well as ion beam assisted deposition (IBAD). Both IBAD and EBAD platinum depositions were carried out *in-situ* without breaking the vacuum. Prior to the milling process the TEM sample was first coated with 10 nm EBAD platinum film followed by a 500 nm IBAD platinum strip. The platinum strip protects the specimen by reducing excessive sacrificial ion etching. The cross sectional TEM was used for the determination of layer thickness and to detail the morphology of the interface region. All imaging and elemental analysis was done on a FEI F30 ST Tecnai operated at 300 kV.

Surface morphology of the sample was studied using a LEO 1550 scanning electron microscope having a field emission gun (FEGSEM) and at an acceleration voltage of 20 kV. In order to avoid charging effects, the samples were sputtered coated with 50 nm of gold/palladium (90/10%).

6.2 Refractive index determination

The derivation of optical constants of semitransparent thin films on a transparent substrate is a well known method from a theoretical point of view [47]. Several approaches can be pursued, but the method used here was to simultaneously fit reflectance and transmittance spectra using the thin film calculation and fitting program CODE (Coating Designer) [48].

6.2.1 Reflectance and transmittance spectra

Semitransparent thin selectively absorbing films of about 50 to 200 nm in thickness, consisting of different volume percentages of nickel ranging from 20 to 80 %, were coated on glass and the reflectance and transmittance spectra between 0.3 to 2.5 μm were measured, according to 6.1.1. Equally thin AR films made of silica, hybrid silica, alumina and silica/titania mixtures were also characterized using the same method.

6.2.2 Simulation and fitting

The optical constants were determined through the use of dispersion and Bruggeman models, see *paper IV*. Measured reflectance and transmittance of thin films on glass substrates, see section 6.2.1, were used to fit the corresponding modeled reflectance/transmittance spectra [49]. The fitting process of, for example, the nickel alumina composite was done using the eight free parameters, six model parameters for the oxide, the thickness and the volume fraction.

6.3 Optimization methods

Studies of the solution-chemically derived selective surface were initiated in a masters thesis work in 2001 [50]. At that time, apart from understanding the process, the work concentrated on a two layer absorber using one solar absorbing base layer and one overlying anti reflection layer.

The optimizing method was mainly experimental and so far iterative in the sense that coatings were deposited with a systematic variation in process parameters, such as concentrations of the solutions, spin coating speed and annealing temperatures and ramping.

After a number of experiments it was found that by using two layers it was impossible to achieve a high enough solar absorptance. Hence the two layer structure was abandoned in favor of a three layer structure made up of two absorbing layers and one AR layer. It was not until the work focused on a three layer absorber that the derivation of the optical properties and refractive indices of the involved thin film materials became necessary. It would be too cumbersome and time consuming to make an experimental optimization of a three layer stack.

When the refractive index of the various single thin films was known, a theoretical three layer structure could be modeled in the thin film program and the optimal three layer absorber could be derived. The program does not

have any automatic fit function that could obtain the highest absorption and lowest emittance. Instead the method was to try manually possible and reasonable three layer stack options, using the materials listed in Table 7.1 and Table 7.2, until an optimum was found. Some guidelines were used for making this optimization: an AR coating is the most effective when its refractive index is equal to the square root of the refractive index of the material it is deposited on, see also section 4.5.1.

The method of optimizing a three layer absorber can be summarized as follows:

1) Determine the optical constants for films prepared under systematically varied process conditions
2) Model an optimal three layer structure using the experimentally determined optical constants in 1).
3) Experimentally prepare a three layer stack using the layer configuration that was selected in 2).

A good reproducibility in the experimental coating process is required for the optimizing method to work.

7 Refractive index

The optical properties and refractive indices presented in this chapter are derived using the method described in section 6.2. The complete and wavelength dependent refractive indices can be found in *paper IV*.

7.1 Nickel-alumina composites

As the nickel content gradually increases both the real and imaginary refractive indices increase, except for the 80% (solution volume percentage) nickel composite, see Table 7.1. The written percentages from now on refer to solution volume percentages. A comparison between the real volume percentage in the solid film and the solution volume percentage can be found in section 9.3.

The nickel nano-particles are heavily absorbing, especially in the solar spectrum. The extinction coefficient exhibits a bulge in Figure 7.1 around 400-700 nm which originates from the non-agglomerated absorptive nickel nano-particles, see Figure 9.1. The composite can be characterized as a dielectric material with a decreasing complex refractive index with wavelength in the near infrared wavelength range for nickel contents between 20-60%.

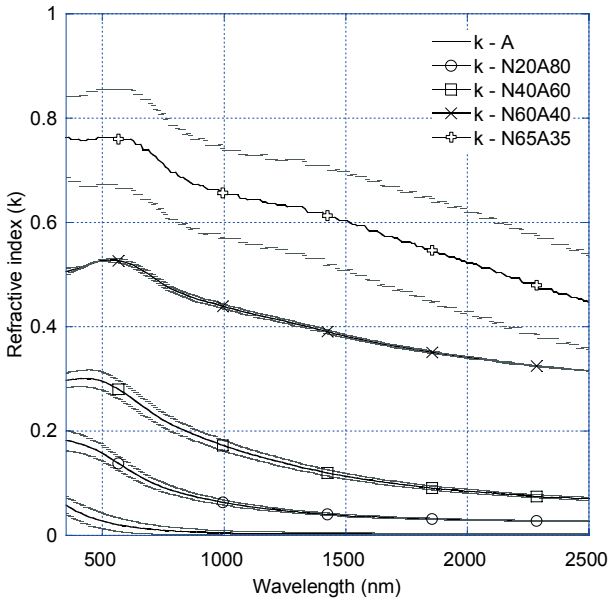

Figure 7.1. The average imaginary part *k* of the refractive index of pure alumina (A) to 65%nickel-35%alumina (N65A35) thin film samples, grey lines represent the standard deviation.

Composites with 65% nickel are on the verge of becoming metallic. For composites with 80% nickel, *k* as well as *n* increase with an increasing wavelength, implying optically metallic behavior. Conclusively, there is a gradual transition to more metallic behavior of the nickel-alumina composite somewhere between a nickel percentage of 65 to 80. However, an absorption bulge can still be seen, but at 700 nm for the 80% nickel samples, which indicates that the nickel particles are still separated. Transmission electron microscopy studies support this assumption, see *paper V*. The TEM images show separated particles even at a nickel percentage of 80%.

Table 7.1. Refractive index at a wavelength of 600 nm for nickel-alumina thin films.

	n (+/-)	**k** (+/-)
20%nickel-80%alumina	1.81 (0.01)	0.13 (0.01)
40%nickel-60%alumina	1.97 (0.01)	0.27 (0.02)
60%nickel-40%alumina	2.17 (0.02)	0.52 (0.01)
80%nickel-20%alumina	2.01 (0.11)	1.23 (0.10)

7.2 AR oxides

Silica is well-known to be a very resilient but static material. In order to make silica more flexible, an organic compound can be incorporated into the glass network structure. The resulting material is called hybrid silica [41]. A flexible material is more likely to perform well in accelerated ageing tests since it is less prone to crack when heated or cooled. According to literature, amorphous alumina has a higher refractive index in the visible wavelength range than amorphous silica, 1.6 compared to 1.4 [37]. Sol-gel derived amorphous titania thin films have a refractive index of 2.0-2.2 in the visible wavelengths and a porosity of 30-40% [38, 39].

The amorphous silica and hybrid-silica thin films heated to 400°C studied here show a constant refractive index over the whole studied wavelength interval, 350-2500 nm. The silica and hybrid-silica films showed no absorption. The studied amorphous alumina thin films heated to 550°C exhibit a slight decrease in the real refractive index with an increasing wavelength. The refractive index of the amorphous 70%silica-30%titania (molar percentage) thin films heated to 500°C is close to that of pure alumina. By increasing the titania content to 50% the refractive index is also increased. The refractive index at 600 nm for the various oxides can be seen in Table 7.2.

Table 7.2. Refractive index at 600 nm for AR oxide thin films.

	N (+/-)	**k** (+/-)
Silica/Hybrid-silica	1.42 (0.02)	0.00 (0.00)
Alumina	1.62 (0.01)	0.02 (0.01)
70%silica-30%titania	1.66 (0.02)	0.03 (0.01)
50%silica-50%titania	1.83 (0.01)	0.05 (0.01)

7.3 Conclusions

The refractive indices of nickel-alumina and silica-titania composites, alumina, silica and hybrid-silica in the wavelength range 350 to 2500 nm were clearly stated and reproducible, apart from the nickel-alumina materials having a nickel content of 65% or more. The nickel-alumina composite behaves as a dielectric up to a nickel content of 60%. There is a gradual transition to more metallic behavior in the nickel-alumina composite when the nickel content increases from 60 to 80 percent by volume.

8 Optimization results

This chapter briefly shows results from absorbers made of a single absorbing layer, one absorbing and one AR layer and finally of two absorbing and one AR layer.

8.1 One layer absorber

The single absorbing layer consisting of nickel particles embedded in an aluminum oxide matrix was thoroughly studied and optimized, see *paper I*. The absorption increased in the solar spectrum interval when the fill factor of nickel was increased up to 60 volume percent, see Figure 8.1. At 80 % nickel the visual appearance of the coating became metal-like and the absorption was instead reduced in the solar spectrum interval. Studies of the optical properties of the nickel-alumina composite confirm this behavior. As discussed in chapter 7, the derived refractive index reveals a transition from dielectric behavior to metallic behavior somewhere between a nickel content of 65 to 80 %.

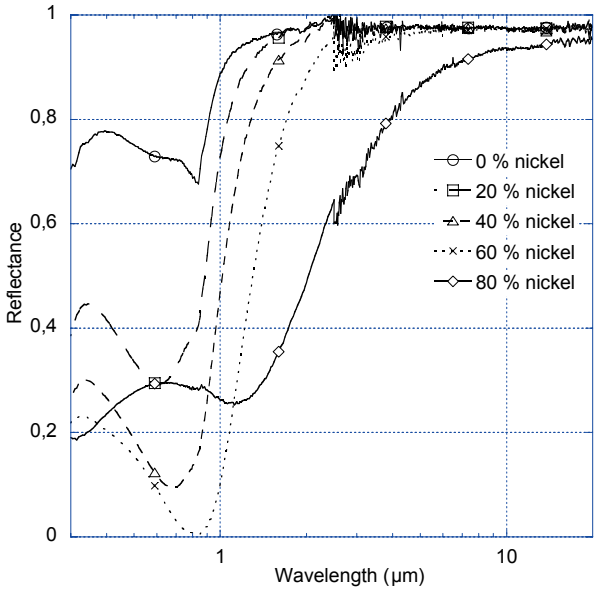

Figure 8.1. Reflectance dependence on different fill factors.

8.1.1 Optimal design

The optimal single absorbing coating had a nickel content of 65 %, a thickness of 0.1 μm and a particle size of 5-10 nm, *see paper I*. The thickness of the film in paper 1 was altered by varying the total metal ion concentration. A higher metal ion concentration leads to a more viscous solution and hence a thicker film. The purchase of a spin-coater with which the spin rate could easily be changed led to the fact that the thickness in later work was mainly varied by changing the spin rate.

Two different types of substrates, optically smooth and rough aluminum, were coated with a spectrally selective surface, see Figure 8.2. More effort was put into finding the optimal coating for smooth aluminum since the surface finish of this type of aluminum is well defined and more consistent than that of rough aluminum.

The best samples were produced with a coating solution of 0.75-0.85 M in total metal ion concentration. As a result the step from low to high reflectance approximately coincides with the ideal transition wavelength, see Figure 3.1. There are two main reasons for the difference in reflectance between optically smooth and rough samples seen in Figure 8.2. The gel does not follow the topography of the surface roughness, instead it fills up the valleys of the rolling groves, resulting in an uneven thickness of the AR layer. The rough surface of the substrate also causes impinging light to scatter in all directions. Hence, the optical interference becomes less pronounced when a rough surface is used as substrate. Smooth samples have typically normal solar absorptance values of 0.80 and normal thermal emittance values of 0.03. The corresponding figures for rough samples are 0.83 and 0.06, respectively.

The heat treatment and the temperature increase rate of the absorbing layer influence the absorptance of the samples, but the effect is not especially significant. On the other hand, the durability was influenced by the heat treatment. The highest temperature increase rate proved to produce the most durable samples, see section 10.3.1.

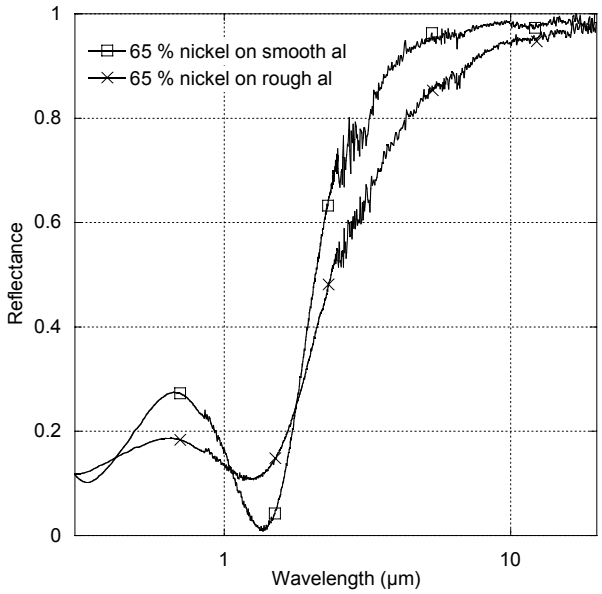

Figure 8.2. Difference in reflectance when using rough or smooth aluminum as substrate.

8.2 Two layer absorber

The two layer absorber consists of one absorbing layer and one AR layer. The refractive index of the absorbing nickel-alumina layer was not yet determined when the work on optimizing a two layer absorber started. The optimal refractive index for the AR material could hence not be computed from thin film calculations. The employed method was instead to test AR materials with different refractive indices and evaluate the result in terms of the resulting normal solar absorptance for the two layer stack.

A base layer made of 65 volume percent nickel heat treated with $50^{o}min^{-1}$ up to 550ºC was coated onto all samples before the AR coating was applied. Five different AR coatings all heated with $50^{o}min^{-1}$ were studied; alumina, silica, silica-hybrid, and two compositions of silica-titania.

It is primarily the constructive optical interference peak at about 0.6 µm, see for instance Figure 8.2, on the one-layer coated samples that is undesirable. An anti-reflection layer of optimal thickness and refractive index suppresses this peak since the interference minimum of the AR coating coincides with the constructive interference of the total layer. As a result, a second interference minimum is acquired at the same wavelength as the former interference

maximum. Adding an AR layer also increases the total film thickness and hence the position of the first interference minimum of the double layer is shifted towards longer wavelengths.

The alumina, silica and hybrid silica AR films have been described in *paper II*. A short summary of those results: Samples coated with alumina (heated up to 580 °C), silica and hybrid silica (550 °C) were quite similar in reflectance behavior, even though they have different refractive indices. The best results were reached with alumina as AR layer. The AR properties for silica and hybrid silica became better with a higher final heat treatment temperature, T_s, but samples coated with pure silica had a tendency to crack as T_s increased, see also Table 8.1.

Paper II consequently showed that the AR material which gave the best optical selectivity was alumina. However, accelerated climate tests showed that alumina is not durable enough, see section 10.3.2. It was then to search for a durable AR material with a refractive index as alumina or higher. Silica proved to be durable, see section 9.3, but has a lower refractive index than alumina. The required properties, durability and correct refractive index, might be obtained by mixing silica with another durable oxide with a higher refractive index, such as titania. Two different mixtures were made, ST73 where the solution molar percentage of silicon and titanium was 70 and 30, respectively, and ST55 with 50 each.

After the experimental work on the two layer absorber, studies of the optical properties of the oxides in question revealed the refractive index, see section7.2. It could be seen that ST73 matches quite well the refractive index of alumina.

The final temperature T_s had the same effect on the silica-titania samples as on the pure silica samples. The optical selectivity increased as the ST samples were heat treated at a higher final temperature. However, as T_s was progressively increased there was a limit when the coatings became prone to cracking. This threshold was seen at temperatures around 530ºC. In order to avoid cracking but still to be able to achieve a good optical selectivity, the final heating temperature was set to 500ºC for the silica-titania samples.

Table 8.1 shows the difference in solar absorptance and thermal emittance for samples coated with the various AR oxides. What can be seen is that the refractive index of the AR material does have an influence on the solar absorptance but it is small, from 0.89 to 0.92.

Table 8.1. Parameters and optical performance for samples before and after an anti reflection treatment. A = alumina, S = silica, HS = hybrid silica (80 mol% TEOS and 20 mol% MTES), ST73 = silica-titania (70 mol% TEOS and 30 mol% TBOT), ST55 = silica-titania (50 mol% TEOS and 50 mol% TBOT)

AR material	A	S	S	HS	HS	ST73	ST55
Al (mol/L)	0.57	-	-	-	-	-	-
Si (mol/L)	-	0.60	0.60	0.66	0.66	-	-
Si+Ti (mol/L)-	-	-	-	-	0.48	0.43	
v_s (rpm)	3700	5000	4000	6000	4000	4000	3000
T_s (°C)	580	350	550	350	550	500	500
ε_{therm} (before)	0.03	0.03	0.03	0.03	0.03	0.03	0.03
ε_{therm} (after)	0.03	0.03	0.03	0.03	0.03	0.03	0.03
α_{sol} (before)	0.79	0.80	0.80	0.81	0.81	0.80	0.80
α_{sol} (after)	0.92	0.89	0.91	0.89	0.91	0.91	0.90
Cracked	No	No	Yes	No	No	No	No

8.2.1 Optimal design

The final conclusion from the AR experiments is that the best optical selectivity that can be achieved with a *two layer* selective absorber based on this nickel-alumina absorber is a normal solar absorptance of 0.92 and a normal thermal emittance of 0.03. The first layer is composed of 65 % nickel and 35 % alumina and the AR layer of pure alumina. However, if the absorber should also be durable it is better to use silica, hybrid-silica or ST73 as AR layer, see section 10.3.2. The absorptance then marginally decreases to 0.91.

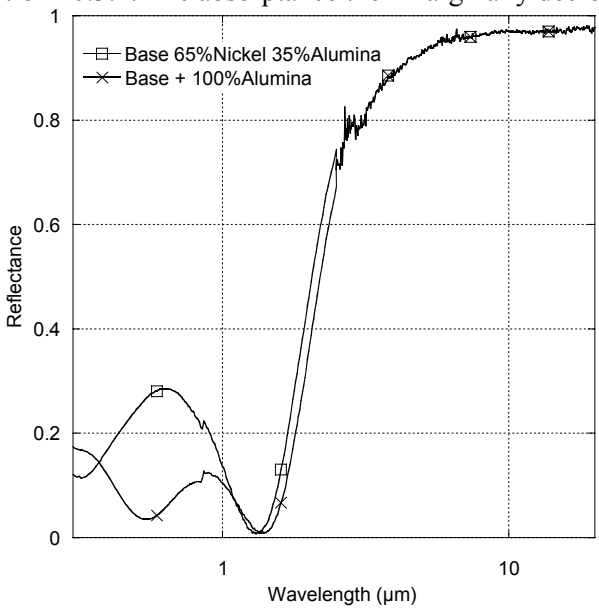

Figure 8.3 Comparison of a sample on smooth aluminum before and after coating with an anti-reflection layer of alumina heated to 580°C.

8.2.2 On optically rough aluminum

The interference effects on rough aluminum are reduced, the interference peak becomes smaller and as a result the effect of the AR coating becomes less noticeable. Only two AR materials, silica and hybrid-silica all heated with 50ºmin^{-1} up to 500ºC were applied to the optically rough substrates. The samples were likely to crack if T_s was set higher. The effect on the reflectance of samples coated with S and HS was very similar. The AR coating decreased the interference maximum of both samples and the resulting reflectance is almost constant at 10 % in the solar spectrum wavelength interval, see Figure 8.4.

An improvement of about 6 % units in normal solar absorptance could be seen, but unfortunately the normal thermal emittance value also increased by about 3 % units. The optimum rough anti-reflection coated sample reached a normal solar absorptance of 0.89 and a normal thermal emittance of 0.06.

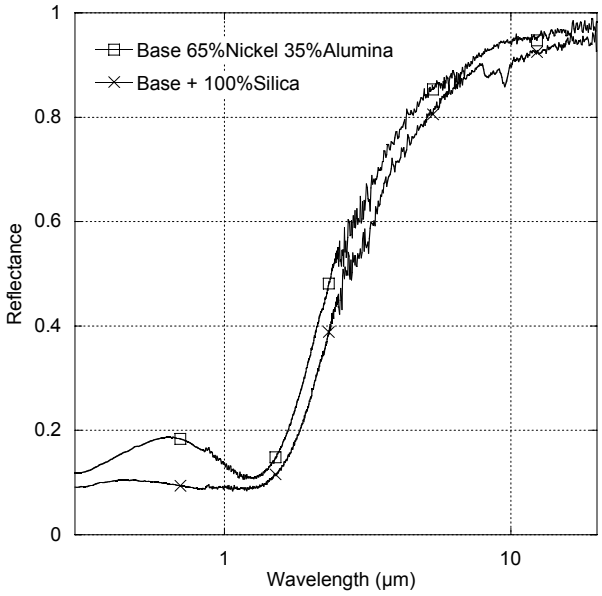

Figure 8.4. Comparison of samples on rough aluminum before and after an anti-reflection treatment with silica heated to 500°C.

8.3 Three layer absorber

Details on the three layer absorber work can be found in *paper III* and *paper IV*. The text below summarizes these results.

8.3.1 Optimized model structure

Simulations based on the optical constants derived in section 7 showed that the optimized three layer selective absorber should be composed of an 80%nickel-20%alumina film of 100 nm at the base, a 40%nickel-60%alumina film of 60 nm in the middle and finally an 100% silica or hybrid-silica film of 85 nm at the top. The modeled three layer stack resulted in a solar absorptance value of 0.97.

8.3.2 Experimental results

A solar absorptance of 0.97 was also confirmed experimentally using this three layer combination found in section 8.3.1. The experimentally made absorbers were produced in three steps. First the aluminum substrate was coated with an 80%nickel-20%alumina solution and heat treated up to 550ºC. Secondly, a 40%nickel-60%alumina was added and the sample heat treated, again to 550ºC. Finally, an AR film of 100% silica was added and the sample received a last heat treatment up to 400ºC.

The reflectance of the sample after the addition of each layer can be viewed in Figure 8.5. The figure reveals that the reflectance is effectively reduced for each additional layer in the solar spectra while remaining relatively unaffected in the IR wavelength interval.

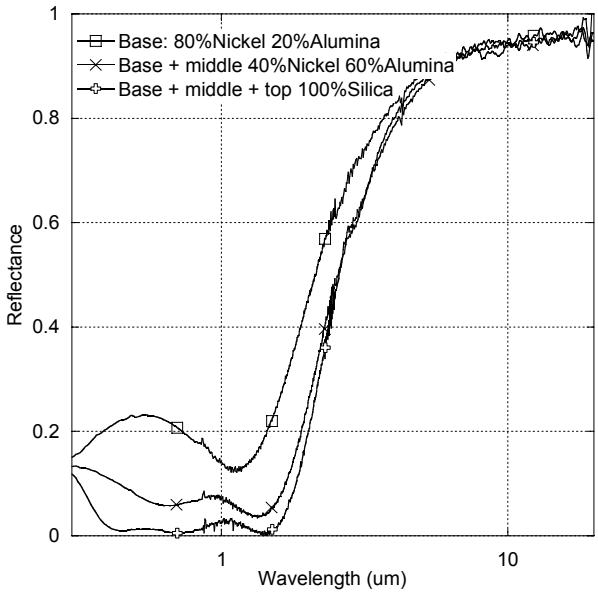

Figure 8.5. Reflectance of the optimized sample after each coating step in the wavelength interval 0.3-20 µm.

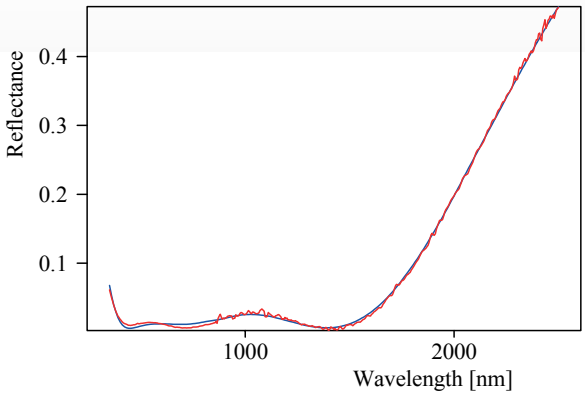

Figure 8.6. Fitted reflectance data for the three layer stack shown in Figure 8.5, the jagged line represents the spectrophotometer data and the smooth line the fit.

It is complicated to obtain the individual layer thicknesses of the three layer absorber experimentally. The thicknesses can be acquired by studying the absorbers using TEM, see section 9.1, but it would be too hard and costly to do that for all samples. More easily the film thicknesses of prepared absorbers could be obtained using the thin film program. The layer composition and the reflectance spectra of the absorber were imported into the program. Then, using an iteration routine and knowing the refractive index of the separate layers, the program fitted the theoretical reflectance to the meas-

ured, see Figure 8.6, using three free parameters, the thicknesses of each layer.

The solar absorptance and thermal emittance values for the one, two and three layer absorbers (presented in Figure 8.5) as well as the individual layer thicknesses for each absorber can be found in Table 8.2. Some shrinkage after each heat treatment can be seen, particularly for the 80% nickel layer.

Table 8.2. Solar absorptance, thermal emittance and individual layer thickness for the absorbers presented in Figure 8.5. The first layer 80%nickel-20%alumina is denoted d_1, the second layer 40%nickel-60%alumina is noted d_2 and the top 100%silica layer is denoted d_3. The theoretically derived modeled optimal thicknesses from section 8.3.1 are added as comparison.

	α_{sol}	ε_{therm}	d_1	d_2	d_3
1 layer	0.79	0.04	112	-	-
2 layers	0.92	0.05	108	61	-
3 layers	0.97	0.05	103	59	90
3 layer modeled	0.97	-	100	60	85

8.3.3 Comments

The method of first theoretically optimizing a three layer structure and transferring the result to an experimental technique worked well. The prepared absorber obtained the same solar absorptance (0.97) as the optimized theoretically modeled three layer stack.

Since there are up to eight free parameters in the fit of the optical constants, see section 6.2, the in this section derived thicknesses might deviate slightly compared with direct measurements using, for example, transmission electron microscopy. White light interferometry (WLI) measurements of individual thin film samples were done in order to confirm the thicknesses of the *single* thin films. Three layer samples could not be measured using WLI. The measured interferometry thicknesses were within ± 5 nm of the fitted single thin film thicknesses. However, the thickness of samples with 80% nickel and samples of pure silica tended to be overestimated by about 20 percent when using the indirect estimates from the optical fit. See more about this discussion in *paper V*.

9 Characterizing results

This chapter summarizes results from *paper V* and *paper VI*. The aim of the electron microscopy study was to investigate by direct measurements the individual layers in terms of layer thicknesses, uniformity, layer boundaries, surface and cross section morphology, particle structure and size. The Elastic Recoil Detection Analysis shows the atomic composition in depth profile.

9.1 Cross sectional morphology

The TEM images represent a visualization of the cross-section in the sense that dense parts, in this case nickel, appear dark and less dense, and alumina appears brighter. Figure 9.1 shows the whole three layer absorber. The individual layers counting from the base of Figure 9.1 are the aluminum substrate and a very thin inter layer of most likely Al_2O_3 from natural oxidation of the aluminum substrate before depositing. The next layers in figure 1 is a 80%nickel-20%alumina layer, a 40%nickel-60%alumina layer and a 100%silica layer. Additionally, two platinum protection layers are clearly visible in Figure 9.1.

The individual films have a completely homogenous composition and adhere very well to the substrate or to each other. The TEM image reveals irregularly shaped grains evenly distributed with a diameter range of 5-10 nm (in the 80% nickel layer) and 3-5 nm (in the 40% nickel layer), see figure 2. The nickel particles are crystalline. Previous X-ray diffraction studies have shown that the alumina is amorphous, see *paper I*.

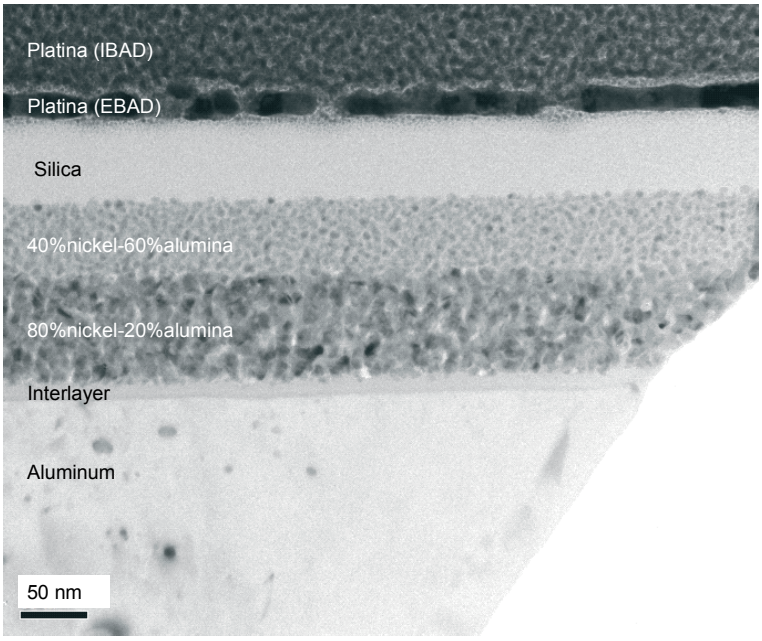

Figure 9.1. TEM image showing a well-defined layer structure of the three layer absorber. Electron and In beam Pt layers are deposited on the surface of the specimen to serve as protective coating for the foil during the milling process.

9.2 Surface morphology

Samples treated with silica cured at 400ºC (S400) and hybrid-silica cured at 400ºC (HS400) and 550ºC (HS550) as AR materials were analyzed by SEM imaging. The SEM images show that micro crack formations could be avoided to a large extent by using hybrid-silica instead of pure silica. Having hybrid-silica generated a smoother surface with fewer cracks compared to pure silica. The final heating temperature also revealed itself to be of great importance for the formation of cracks and surface morphology. Hybrid-silica heated to 400ºC shows larger formations with nano cracks in the surface morphology. Silica and hybrid-silica heated to 400 and 550°C respectively exhibit a more granulated surface morphology.

The dominating reason for film cracking is film shrinkage during the heating process [51]. The solidification process is initiated at low temperatures with evaporation of solvents and H_2O, at this stage there is not that much shrinking. The main part of the shrinking occurs at higher temperatures due to condensation of Si-OH bonds. In the last stage organics are oxidized and there is a further densification of the structure. Note that these three processes; evaporation, condensation and oxidation do not occur completely separated

but overlap in time and temperature. The difference in the thermal expansion rate between the densified film material and the underlying aluminum substrate can also contribute to cracking in the subsequent cooling, but is almost always not as important [51].

9.3 Elemental depth profile

Figure 9.2a shows the ERDA relative atomic depth distribution of a three layer absorber with S400 as AR layer. The depth scale for this technique is areal density in units of 10^{15} atoms/cm^2. In Figure 9.2b a TEM image of the same sample is fitted to the ERDA profile in order to see more easily where the layer boundaries are. The steps in, for example, the oxygen level also indicate where the layer boundaries are.

It was found that the oxygen to silicon relation in the anti reflection silica, both pure and in hybrid form was slightly higher than 2:1. The same trend was seen for the alumina in the base and middle nickel-alumina layers of the absorber, a higher oxygen to aluminum relation than 3:2. The higher oxygen content in both the silica and alumina layers could be due to some residual H_2O and OH groups. However, the overrepresentation of oxygen in the nickel-alumina layers is more likely explained by surface oxidation of the nickel nano particles.

Apart from Si, Ni, Al and O, small impurity levels of nitrogen, carbon and hydrogen could be detected. The nitrogen contamination of about 1% might stem from the heating process where nitrogen was used as atmosphere. The hydrogen and carbon content of about 1 to 3% and 2 to 4%, respectively, all throughout the silica and nickel-alumina layers, originates from residual H_2O, OH and carbon in the films. There is an evident difference in the carbon and hydrogen content between silica and hybrid-silica. It is the added carbon and hydrogen containing methyl groups in hybrid-silica that make the silica structure more flexible and durable that explains the difference.

A study of the difference between solution volume percent and actual volume percent was also made using ERDA. Individual nickel-alumina films with varying ratios coated on glass substrates were investigated. The result showed that the difference is very small for low nickel percentages. For high nickel percentages the ERDA measured nickel volume percentage is up to three percent higher than in the solution. The ERDA measurements also indicate that about 15% of the nickel found in the nickel-alumina composite films is bound in the form of NiO. For full details of the ERDA investigation, see *paper VI*.

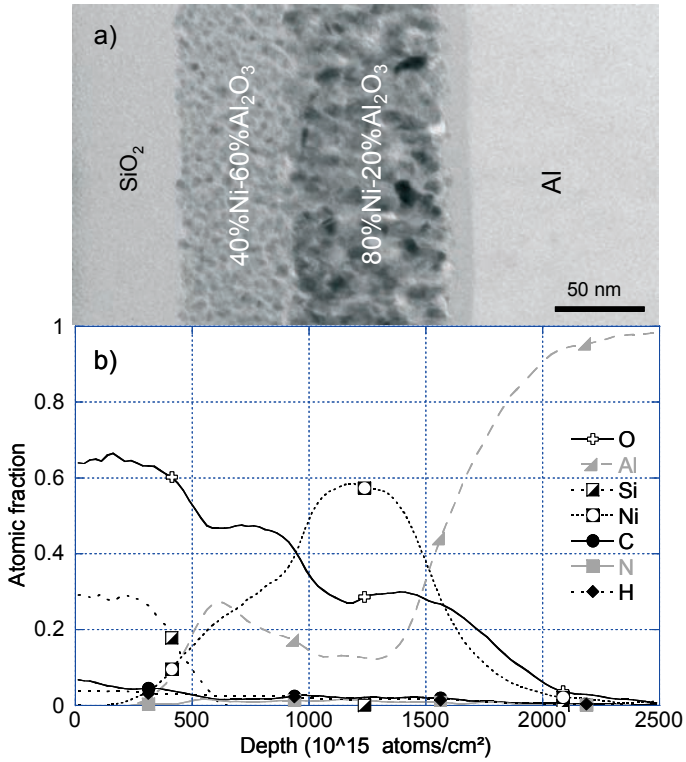

Figure 9.2. (a) Cross sectional profile of a three layer absorber obtained by TEM. (b) Relative atomic depth profile of the same sample measured by ToF-E ERDA.

9.4 Conclusions

The TEM investigation confirms that the used absorber model resembles the real structural properties of the composite coatings. It was found that the thickness uniformity is excellent and that the layers are smooth and exhibit none or very small layer intermixing. This explains why the optimization method using the absorber model, based on effective medium theory and Fresnel formalism for smooth and uniform surfaces, works so well and that optical interference can be used to design the solar selective coating. The absorbing coatings contain distinct metal particles of crystalline nickel of sizes in the range 3 to 10 nm. SEM images show that micro crack formations could be avoided to a large extent by using hybrid-silica instead of pure silica. Durability tests have also shown that a hybrid-silica AR coating is slightly more stable at high temperatures than pure silica, see section 10. The ERDA study confirms the layer structure and shows that the solution volume percentage is almost identical with the real volume percentage.

10 Accelerated ageing

A solar thermal collector generates what could be called a micro climate. The absorber will encounter stagnation temperatures of about 200ºC as well as high humidity and condensation conditions. The micro structure of a thin coating is not permanent over time. Factors such as high temperature, high air humidity, airborne pollutants and sun radiation can cause the coating to deteriorate and hence affect the optical selectivity of the surface [52]. High temperatures can speed up oxidation processes and high levels of humidity may create hydrolytic reactions, i.e. electrochemical corrosion. Airborne pollutants might also accelerate electrochemical corrosion processes and solar radiation can initiate photochemical redox reactions. A combination of these processes can be devastating for a large number of materials, including solar selective coatings.

The most accurate method used to test the durability of a solar absorber is to assess it under normal working conditions. These so-called in-situ tests are however very hard to carry out because of the time length required to get results. Instead of exposing the absorber surface to its natural working conditions for many years, laboratory tests can be done in a climate chamber, where temperature and humidity can easily be controlled. The temperature and/or the humidity in the chamber can be elevated in order to accelerate ageing.

The micro and nano surface structures influence the durability of the selective solar absorber. The denser, crack free and inert the film is the better it will perform in accelerated ageing tests.

10.1 Equipment

To perform accelerated condensation tests a Vötsch Industrietechnik climate chamber of type VC 4033 MH was used. It is possible to run tests within a temperature range of 25 to 90°C in the chamber while regulating the relative humidity between 10 to 95 %. The sample holder was water-cooled to ensure that condensation was formed on the samples. A thermostat bath of type Techne Tempunit TU-16D ensured that the temperature of the cooling water was about five degrees lower than the temperature of the chamber.

The accelerated high temperature tests were performed in a Vecstars Furnaces, type ECF2 furnace.

10.2 Testing procedures

Condensation, high temperature and aggressive airborne pollutant tests are recommended for solar absorber coatings. It is especially important to perform the condensation test on the type of absorbers investigated in this work because previous experience shows that alumina can be sensitive to moisture [53]. The high temperature test can reveal if the nickel nano-particles are susceptible to oxidation. To be able to compare accelerated ageing test results from different laboratories, some kind of test procedure has to be defined. There is no European standardized procedure for testing the durability of a solar absorber surface, but some assessment methods have been proposed by the International Energy Agency, IEA [54]. More about these test methods can be found in *paper VIII*.

The condensation test was performed according to IEA SHC Task 27 criteria [54]. In the condensation test, samples were subjected to two temperature levels of 45 or 65°C and a relative humidity of 95 %. The tested samples were cooled 5º below ambient to ensure condensation upon the sample surface. Tested samples were assessed according to the following performance criterion (PC):

$$PC = -\Delta\alpha_{sol} + 0.5\Delta\varepsilon_{therm} \leq 0.05 \qquad \text{Equation (10.1)}$$

where $\Delta\alpha_{sol}$ is the difference in normal solar absorptance before and after the test and $\Delta\varepsilon_{therm}$ is the difference in normal thermal emittance. The factor 0.5 reduces the importance of a change in thermal emittance compared to a change in solar absorptance. Previous proposed test criteria by the IEA SHC Task X [52] used a weighting factor of 0.25 for thermal emittance but a factor of 0.5 was found to be more appropriate by Task 27. The testing cycle should continue up to 600 hours as long as the *PC* value is less than 0.05, if not, it is terminated. Note that it is possible to get a negative *PC* value, which indicates an actual improvement of the optical selective properties of the surface. If the *PC* value is greater than 0.05 after 600 hours at 40ºC the samples should be tested and evaluated at 60ºC.

In the high temperature assessment the test temperatures are determined by the pre test performance of the absorber, the better the absorptance and emittance values are, the higher the test temperatures become [54]. Absorbers

with 0.97 in absorptance and 0.05 in emittance should first be evaluated at 290ºC. The PC-value should be evaluated after t_1=18, 36, 75, 150 hours. If the PC value is greater than 0.05 after t_1 hours the sample should instead be tested at 260ºC for t_2=97 hours. If PC (260ºC, t_2) ≤ (290ºC, t_1), the absorber is qualified.

Aggressive airborne pollutant tests were not performed within this thesis work but will be dealt with in the near future.

10.3 Condensation test results

10.3.1 One layer absorber

The tests showed that the temperature increase rate strongly influenced performance. The higher the temperature increase rate, the better the absorber performed in the accelerated ageing test. Samples made with the lowest temperature increase rate showed strong absorption in the infrared wavelength range. The infrared absorption is mainly due to oxo- and hydroxo-groups that are formed when H_2O reacts predominantly with aluminum. The reflectance curve of samples treated with a higher temperature increase rate was not affected as greatly. The surface appearance however became slightly rough and the transition from low to high reflectance was shifted towards shorter wavelengths, see Figure 10.1a and b. For more details see *paper VII*.

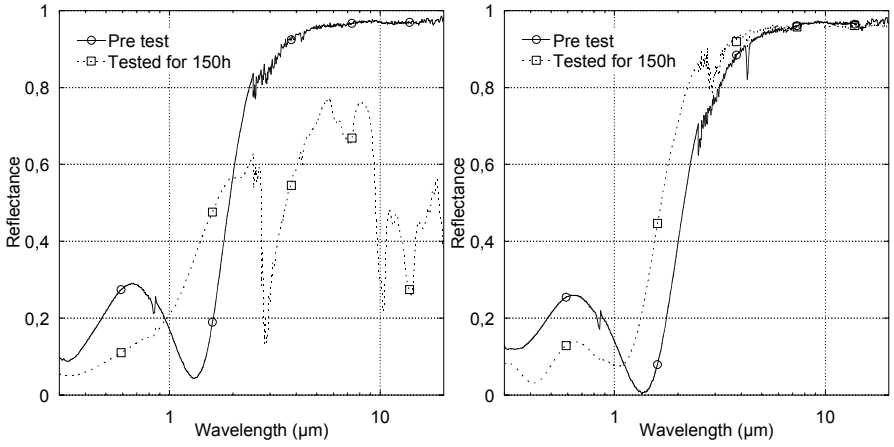

Figure 10.1 a and b. Comparison of samples before and after 150 hours of an accelerated ageing test. (a) heated with 5ºmin^{-1} up to 580ºC (b) heated with 60ºmin^{-1} up to 580ºC.

10.3.1.1 Rough aluminum substrate

Rough samples did not perform as well as smooth samples, even though they were made under the same conditions. The appearance of the surface itself had changed and strong absorption of infrared radiation could be seen. The surface itself became duller and whitish. The trend that the samples became more durable the higher the temperature increase rate they were treated with was also clearly seen for rough aluminum specimens.

10.3.2 Two layer absorber

A base layer made of 65 volume percent nickel had been coated onto all samples before the AR coating was applied. (The only exception was the base layer for the alumina coated sample which has a 70 % nickel base layer heat treated with 30 °min^{-1} up to 580ºC.) The parameters ε_{therm}, α_{sol} and PC for the aged samples can be found in Table 10.1 and more details in *paper VII*.

The reflectance curve of the absorber coated with alumina AR film, tested for 80 hours, already showed strong absorption bands in the infrared, see Figure 10.2a, and consequently the normal thermal emittance value drastically increased.

All other AR materials, silica hybrid-silica and silica-titania proved to be very resilient. Minor or no changes at all to the optical performance were seen, even after 600 hours of testing. It could be seen that the hybrid silica samples were more resilient than the corresponding silica samples. A hybrid-silica sample tested for 600 hours can be seen in Figure 10.2b.

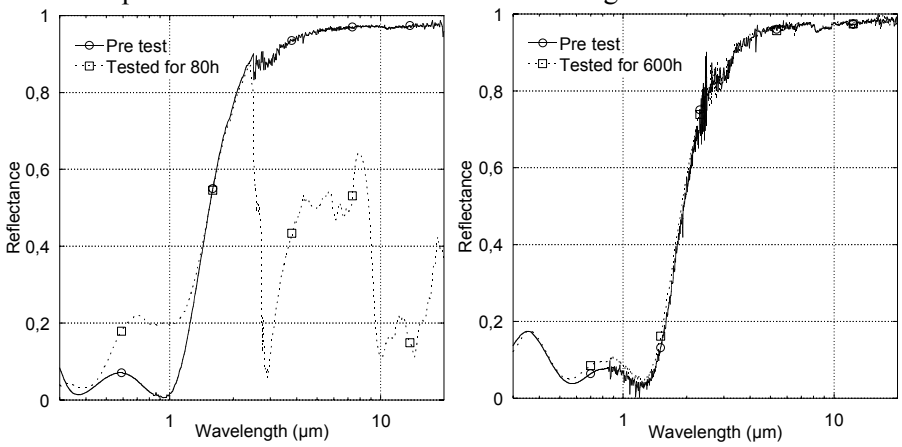

Figure 10.2a and b. Comparison of samples before and after an accelerated ageing test. (a) coated with A, heated to 580ºC and tested for 80 hours (b) coated with HS, heated to 350ºC and tested for 600 hours.

Table 10.1. Normal solar absorptance, normal thermal emittance and performance criterion values of accelerated lifetime tested samples. A = alumina, S = silica, HS = hybrid silica (80 mol% TEOS and 20 mol% MTES), ST73 = silica-titania (70 mol% TEOS and 30 mol% TBOT).

AR material	A	S	S	HS	HS	ST73
T_s (°C)	580	350	550	350	550	500
ε_{therm} (0h)	0.03	0.03	0.03	0.03	0.03	0.03
α_{sol} (0h)	0.91	0.88	0.90	0.89	0.90	0.91
ε_{therm} (80h)	0.59	0.03	0.05	0.03	0.03	0.04
α_{sol} (80h)	0.76	0.86	0.89	0.88	0.90	0.91
PC	0.21	0.02	0.02	0.01	0.00	0.00
ε_{therm} (300h)	-	0.04	0.07	0.03	0.04	0.05
α_{sol} (300h)	-	0.86	0.89	0.88	0.90	0.91
PC	-	0.023	0.02	0.01	0.00	0.01
ε_{therm} (600h)	-	0.04	-	0.03	-	-
α_{sol} (600h)	-	0.86	-	0.88	-	-
PC	-	0.02	-	0.01	-	-

10.3.2.1 Rough aluminum substrate

A base layer made of 65 volume percent nickel, heat treated with 50 °min^{-1} up to 550ºC, had been coated onto all samples before the AR coating was applied. The parameters ε_{therm}, α_{sol} and *PC* for the aged samples can be found in Table 10.2. Two samples with each type of coating were subjected to the condensation test. Only silica and hybrid silica were tested in this section.

The silica coated absorber tested for 80 hours appeared to be severely affected and the reflectance curve also showed strong absorption bands in the infrared, see Figure 10.3a. The normal thermal emittance value drastically increased and the normal solar absorptance value decreased from 0.89 to 0.84. The performance criterion became 0.10 which exceeds the limit, thus further testing was unnecessary. On the other hand the hybrid silica coated sample was virtually unaffected after 80 hours of testing and it was tested for another 220 hours. The reflectance curve after 300 hours revealed that the HS sample too had been affected by the test. Large infrared absorption bands were evident but the reflectance in the solar wavelength range was close to unaffected, see Figure 10.3b.

Again the HS coating proved to be more resistant towards the accelerated ageing test. The difference in test results between silica and hybrid-silica are however greater for rough compared to smooth samples.

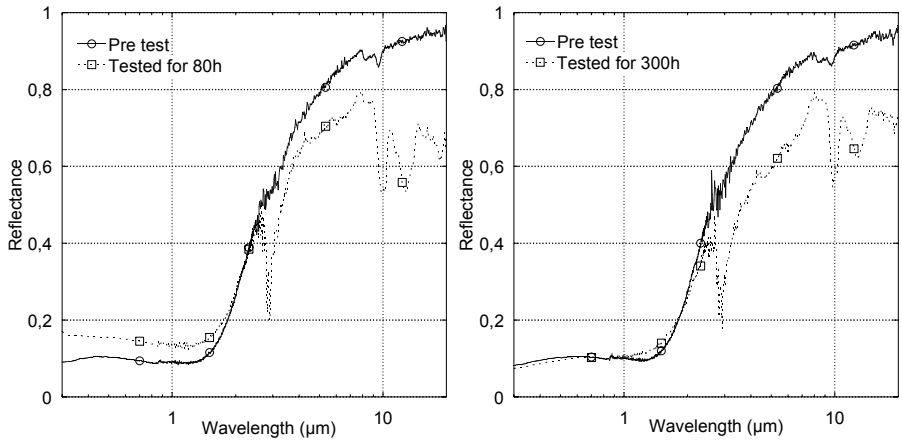

Figure 10.3a and b. Comparison of samples before and after an accelerated ageing test. (a) coated with S, heated to 500ºC and tested for 80 hours (b) coated with HS, heated to 500ºC and tested for 300 hours.

Table 10.2. Normal solar absorptance, normal thermal emittance and performance criterion values of accelerated lifetime tested samples.

AR material	S	HS
T_s (°C)	500	500
ε_{therm} (0h)	0.09	0.09
α_{sol} (0h)	0.89	0.88
ε_{therm} (80h)	0.29	0.09
α_{sol} (80h)	0.84	0.88
PC	0.10	0.00
ε_{therm} (300h)	-	0.28
α_{sol} (300h)	-	0.88
PC	-	0.05

10.3.3 Three layer absorber

All three layer absorbers were made up of one 80% nickel base layer and one 40% nickel middle layer. The differences lie in the structure and composition of the third AR layer. The AR coating was altered between pure silica heated to 400°C and hybrid-silica heated to either 400 or 550ºC. The two layer study, see section 10.3.2 showed that samples coated with hybrid-silica perform just as well or even better than silica coated samples in this kind of test. Hybrid-silica coated samples were thus not condensation tested.

The samples were practically unaffected after a 600 hour condensation test at 40ºC and 95% RH and hence the three layer absorber qualified well accord-

ing to the Task 27 guidelines [54]. More details about the three layer condensation test results can be found in *paper VIII*.

10.4 High temperature test results

Only the complete three layer absorber was high temperature tested. Again as in section 10.3.3 the only varying parameter between the samples was the AR layer, silica heated to 400°C or hybrid-silica heated to 400 or 550°C.

No sample passed the performance criterion after 18 hours of testing at 290°C, see Table 10.3. However, after 97 hours of testing at 260ºC all samples showed a lower or equal PC value than at 290°C. Consequently, all samples qualified, according to the test procedure described in section 10.2. The material that qualified with the greatest margins was the hybrid-silica heated to 550ºC, see Figure 10.4 and Table 10.3. More details about the high temperature three layer test results can be found in *paper VIII*.

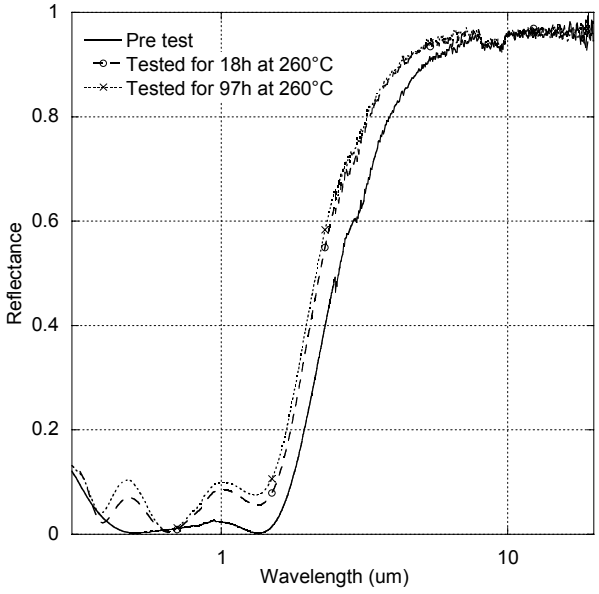

Figure 10.4. A hybrid-silica coated absorber heated to 550°C and tested at 260°C.

Table 10.3. Normal solar absorptance, normal thermal emittance and performance criterion values of high temperature tested samples. S = samples with silica as AR layer, HS = samples with hybrid-silica.

AR material	**S**	**HS**	**S**	**HS**	**HS**	**S**	**HS**
Test temp. (ºC)	200	260	260	260	290	290	290
T_s (°C)	400	400	400	550	400	400	550
ε_{therm} (0h)	0.063	0.048	0.057	0.052	0.048	0.057	0.052
α_{sol} (0h)	0.965	0.967	0.962	0.968	0.967	0.962	0.968
ε_{therm} (18h)	-	0.038	0.039	0.043	0.036	0.035	0.047
α_{sol} (18h)	-	0.906	0.902	0.926	0.881	0.889	0.884
PC	-	0.056	0.042	0.038	0.080	0.062	0.082
ε_{therm} (97h)	-	0.042	0.032	0.042	-	-	-
α_{sol} (97h)	-	0.892	0.890	0.910	-	-	-
PC	-	0.072	0.060	0.053	-	-	-
ε_{therm} (200h)	0.065	-	-	-	-	-	-
α_{sol} (200h)	0.963	-	-	-	-	-	-
PC	0.004	-	-	-	-	-	-

10.4.1 Elemental depth profile

ERDA measurements of the three layer samples were carried out before and after the high temperature test, to see if the elemental depth composition had changed. The most evident change before and after the high temperature testing independent of the AR coating material is seen in the oxygen and nickel content. The relative oxygen content is clearly higher in the 40%nickel-60%alumina and the 80%nickel-20%alumina layers, indicating that oxidation has taken place. A reduction of the relative nickel content in the 80%nickel-20%alumina layer can also be seen. According to Figure 10.4 there is no formation of hydroxo compounds (no absorption in the IR) and thus the degradation can be completely assigned to oxidation of the nickel.

The oxidation of nickel particles explains the drop in absorptance seen in Table 10.3. The same table also shows that oxidation is only active during the first hours of the high temperature test. The relative reduction of nickel and the increase in oxygen is the least pronounced for the hybrid-silica sample heated at 400°C. More details can be found in *paper VIII*.

11 Concluding remarks

A novel way of manufacturing spectrally selective solar thermal absorbing surfaces was investigated, developed and optimized. The absorbing material consists of nickel nano-particles in an alumina matrix. Anti-reflection coatings made of silica, hybrid-silica, alumina and titania were used to improve the performance. The optimizing approach was initially experimental when a two layer absorber was developed which achieved a normal solar absorptance of 0.92 and a normal thermal emittance of 0.03. To be commercially interesting an absorptance of 0.94 or more is needed. Hence a three layer absorber was studied. In order to optimize a three layer stack, the refractive indexes of the thin film materials were obtained and the optimal three layer configuration could then be modeled theoretically. The theoretical stack was experimentally confirmed and achieved a solar absorptance of 0.97 and a thermal emittance of 0.05, which are definitely commercially competitive values.

The thin film absorbing and anti reflecting materials were characterized using reflectance, TEM, SEM and ERDA measurements. Through the use of these techniques the refractive index, surface and cross sectional morphology, elemental depth profile and the absorption and emission properties could be obtained. A homogenous layer structure with a very small or no layer intermixing was found. The layers were even in thickness with minor surface roughness. Nickel nano-particles of 3-10 nm were seen. The characterizing results validate the theoretical optimization which was based on the model of the absorber surface assuming that the layers do not intermix and are homogenous, and that the nano-particles are much smaller than the wavelength of visible light.

Accelerated ageing tests have revealed that providing the AR coating is made of durable and dense silica or titania the three layer absorber qualified according to the new proposed IEA standard. The condensation test did not degrade the absorber whatsoever, but the high temperature tests revealed some oxidation of the nickel particles. The oxidation occurred initially in the high temperature test and then stopped. The formed nickel-oxide layer hindered further oxidation. Hybrid-silica proved to be slightly more durable than pure silica. Accordingly, SEM images showed less cracking in hybrid-silica than in ordinary silica.

This thesis shows that the solution-chemical method could produce highly selective and durable selective surfaces. Advantages of the technique are: it is simple and easy to control the process, the coating can be manufactured under ambient pressure conditions and the process is low in material consumption. The method seems promising and could hopefully reduce production costs for spectrally selective absorbers and hence make them less expensive and more available.

In order for solar thermal systems to be more acceptable it is of vital importance that the solar fraction is increased and the cost decreased. If the solution-chemical absorber can lower the cost of the solar collector it would be a step in the right direction. The solar fraction can be improved through a number of technical modifications of the system, such as the use of concentrating systems. People selling or handling the system up to installation are very important who should optimize the solar thermal system to the needs and conditions of the user. How the system is used once it is installed is also essential. Different users can merely by their operation load profile affect the solar fraction of an identical thermal solar system.

Using solar energy instead of fossil fuels or electricity is an excellent way of decreasing our negative impact on the environment. Solar thermal devices still cannot supply enough heat during the coldest months at high latitudes, so an auxiliary source, preferably one as carbon dioxide neutral as possible, is needed. But even in places on as high latitude as Uppsala, DHW solar fractions of up to 70% are easily achievable without risking overheating of the solar thermal system. To conclude; as electricity, oil and gas prices are on the rise the future of solar energy definitely looks bright.

12 Future outlook

This chapter discusses up-scaling issues of the developed solution-chemically derived patented absorber. Collaboration with an industrial partner has been initiated. This work is focused on designing, constructing, optimizing and running a pilot-plant that will produce a solar thermal absorber which uses the selective surface developed in this thesis.

The material costs for a three layer absorber are less than 3 SEK per square meter which can be reduced further if the solvents used in the process are recycled. However, the price of the aluminum substrate is around 35 SEK per square meter for the rough variant and about 90 SEK per square meter for the smooth variant. Consequently, the material costs for coating itself are negligible compared to the cost of the substrate. As a comparison, the material cost for a thickness sensitive spectrally selective paint is around 2 SEK per square meter [31].

The costs for the production process and heat-treating have not been estimated. But since similar processes are already in use within the industry it should not be too costly to construct and operate a well running production process adapted to this solution-chemistry technique. Before coating can take place some form of substrate cleaning is required. There are already several in-line adaptable cleaning techniques that could be suitable for this process.

Spin-coating processes are easy to handle but there is one considerable disadvantage. This technique is not suitable for large surfaces. Instead two other wet coating methods could be of practical interest for industrial use, spray- and dip-coating. Spray-coating techniques are quick and easily adaptable to different coating solutions. Complex shapes can be coated, suitable for the establishment of an in-line process, and there is a minimum of material waste. One shortcoming is that one nozzle can coat only one surface at a time. Dip-coating processes are simpler and coat two sides at the same time but they are slow and the material waste is greater. The number of advantages of the spray-coating method suggests that this is the preferred technique when up-scaling the process. The feasibility of spray-coating the AR layer of the solar absorber was investigated [55]. The obtained results show that it is indeed possible to obtain thin films in the range below 100nm, of

sufficient surface quality. But it also became clear that some challenges do exist with regard to this method. One challenge was to obtain a homogenous thickness over a large area. Newly performed tests (summer of 2006) using electrostatic spray-coating show a largely improved thickness uniformity thanks to the fact that the electrostatic forces are much stronger than merely gravity. The spray-coating experiments have showed that it is important to work with slow evaporating solvents in the solutions. Fast evaporating solvents will evaporate too quickly, sometimes even before the spray reaches the substrate and as a result only dry powder hits the substrate. By utilizing spray-coating the film structure on a rough substrate will also most probably be changed. It could be expected that the undesired effect of spin-coating that the film becomes thicker in the valleys and thinner on the top of the rolling groves would decrease when spray-coating is used but more tests on rough substrates have to be performed.

The heat treatment technique has to be redesigned. It is impractical to place a large coated sample in an airtight box, seal the box and then heat it. It is better to construct a method that is adaptable for an in-line production process. Possible heating methods could use near infrared radiation, microwaves or laser assisted heating. The necessary non-oxidizing environment could be created by ensuring overpressure of nitrogen along the whole heating part of the production line. Furthermore, if the process is to be feasible, a high temperature increase rate is required, as otherwise the length of the heating and cooling zone will be too long.

13 Acknowledgements

First of all I would like to thank my excellent supervisor Prof. Eva Wäckelgård, who came up with the idea that led to this study, for her invaluable support and for giving me the creative freedom that I so much appreciated. Prof. Gunnar Westin deserves a lot of credit for his guidance and for letting me use the technique. I would like to express my gratitude to Dr. Annika Pohl and Dr. Åsa Ekstrand for providing me with Ni-Al solution help and their never-ending patience.

I would also like to express my appreciation to:
The Energy Systems group and especially Mari-Louise Persson, Magdalena Lundh, Fredrik Karlsson, Wiktoria Glad, Charlotta Isaksson, Anna Werner and Andreas Jonsson for many interesting discussions, lunches, excursions and enjoyable collaborations. Björn Karlsson for being full of ideas and coming up with new concepts. The whole Task 28 working group and especially Johan Smeds, Maria Wall, Robert Hastings and Daniela Enz. Arne Roos for helping me with measurement problems and fixing broken spectrophotometers. Bengt Peres for his support with the simulation tool WINSUN. Those who make sure that the all other equipment works, Shuxi Zhao, Bengt Götesson, Jonatan Bagge, Mikael Österberg...

My co-authors Jens Jensen, Sima Valdizadeh and Jun Lu for fruitful collaboration. All former and present members of the Solid State Physics group for their backing and encouragement. Michael Köhl and his group in Freiburg at the Fraunhofer Institute for Solar Energy Systems for taking me in and letting me work in his group during an exchange stay in 2005.

But most of all I would like to thank my parents, siblings and friends! Without your friendship and all the things we do together, whether it be chatting, climbing, building houses, skiing, riding ass-notes or just enjoying each other's company and having fun, you should know that all this would have been impossible if it were not for you!

The work has been carried out under the auspices of the Energy Systems Programme, which is financed by the Swedish Foundation for Strategic Research and the Swedish Energy Agency.

14 Sammanfattning på svenska

Det här kapitlet beskriver kortfattat min forskning kring solabsorbatorytor och solvärmesystem. Hur kom jag då in på det här? Det hela började med att jag vid sju års ålder började titta på tv. Program som visade jordens alla problem med bland annat växthuseffekten, nedsmutsning, svält samt vatten- och energibrist blixtrade fram på rutan. Som barn trodde jag då att man kunde lösa många av dessa problem genom att hitta DEN ultimata energikällan. Föreställ dig vad mycket gott du skulle kunna göra om man hade tillgång till en oändlig hållbar energikälla! Då på åttiotalet stod hoppet till fusionskraft och jag ville följaktligen bli fusionsforskare. Men på tvåtusentalet blev jag mer intresserad av en enklare teknologi, den mer lättillgängliga solenergin vilken faktiskt baseras på just en enorm fusionsreaktor, bara placerad ett par hundra miljoner kilometer ifrån oss. Nu står jag här år 2006 med en ny doktorsavhandling som förhoppningsvis bidrar till att föra solenergitekniken ännu ett steg framåt.

Ett samhälle som bygger på fossila bränslen utgör inget hållbart samhälle. För att minska vår åverkan på jorden behövs miljövänliga alternativ, ett sådant alternativ är solenergi. Jorden tar årligen emot tusentals gånger mer energi i form av instrålat solljus än vad världen använder. Att fånga in solenergi och konvertera den till värme möter inga hinder, problemet ligger i lagringen av energin. För att solvärme ska bli effektivare och därmed få en ökad acceptans måste bland annat täckningsgraden för solvärme öka. Täckningsgraden kan höjas med hjälp av ett antal olika tekniska modifieringar av systemet men lika viktigt eller viktigare i sammanhanget är användningen och brukaren av det tekniska systemet. Det är grundläggande att ha en bred systemsyn för att ett tekniskt system som till exempel ett solvärmesystem i realiteten ska fungera optimalt.

Det finns i princip tre olika typer av solfångare: plan, vakuum samt koncentrerande solfångare. Den viktigaste delen av solfångaren består av en svart platta kallad absorbatorn, inbyggd i ett isolerat utrymme och skyddad av ett yttre hölje. Solstrålning träffar absorbatorn och ljusenergin övergår till värmeenergi. Genom absorbatorn strömmar ett värmemedium som upptar och leder bort värmeenergin till en lagringstank. Ett tvärsnitt av en plan solfångare kan ses i figur 2.1.

Min avhandling är uppdelad i två avdelningar, en huvuddel rörande solfångarens hjärta – den spektralt selektiva absorbatorytan och en del rörande solvärmesystem. De bifogade artiklarna behandlar utvecklingen och karakteriseringen av absorbatorytan. Publikationer rörande solvärmesystem har inte bifogas till avhandlingen.

Den dominerande delen av min tid som doktorand har gått till att utveckla, optimera och karakterisera av en ny typ av spektralt selektiv absorbatoryta, baserad på lösningskemi. Syftet med detta projekt var att undersöka potentialen av denna nya absorbatoryta. Till en början fanns ett antal frågeställningar, bland annat; skulle det gå att framställa en lämplig absorbator med den nya lösningskemiska metoden, hur hög verkningsgrad var möjlig, skulle absorbatorytan bli bättre med hjälp av en antireflexbehandling, hur många lager och vilka lager skulle absorbatorn bestå av, kommer absorbatorn att bli klimatbeständig och hur beskrivs och ser absorbatorytan ut på en nanoskala? Absorbatorn är uppbyggd av spektralt selektivt absorberande tunnfilmer bestående av nickelnanopartiklar i aluminiumoxid och ett antireflexskikt bestående av kiseloxid, hybridkiseloxid, aluminiumoxid eller en blandning av kisel- och titandioxid. För att tillverka de olika tunnfilmerna använde jag lösnings- och sol-gel-kemi. Lösningarna belades på aluminiumsubstrat med hjälp av spin-beläggning. Slutligen värmebehandlade jag proverna för att förånga lösningsmedlen, tunnfilmen stelnar då och antar sin slutliga form.

Jag har bestämt de optiska konstanterna för de ingående tunnfilmsmaterialen. Den optimala solabsorbatorytan i form av en trelagerstruktur har sedan modellerats fram med hjälp av dessa optiska konstanter. Jag har verifierat den teoretiskt framtagna trelagerstrukturen experimentellt och uppnådde då en solabsorptans av 0.97 och en termisk emittans av 0.05. Dessa värden visar att den nya absorbatorytan med marginal är kommersiellt konkurrenskraftig. En ideal solabsorbatoryta har 1 i solabsorptans och 0 i termisk emittans. De tre lagren består av en 80%nickel-20%aluminiumoxid film i botten, en 40%nickel-60%aluminiumoxid film i mitten och överst en kiseloxid eller hybridkiseloxid film. Den totala tjockleken för de tre lagren är cirka 200 nm. För att kunna studera hur pass beständig och hållbar den nya absorbatorytan var utförde jag accelererade klimattester enligt ett testschema utvecklat av IEA Task 27. Två varianter utfördes, en högtemperatur- och en kondenstest. Absorbatorn klarade kondenstesterna utan någon synlig eller mätbar degradering men efter högtemperaturtesten syntes en viss oxidation av nickelnanopartiklarna. Oxidationen sker tidigt i testen men avstannar snabbt då det bildas ett nickeloxidskikt på partiklarna som skyddar mot fortsatt oxidering. Graden av oxidering är liten och absorbatorytan är kvalificerad enligt Task 27's test procedur. Ett samarbete med en industriell partner har inletts och förhoppningen är att den nya patenterade absorbatorytan ska finnas tillgänglig för marknaden om några år.

15 References

[1] www.stem.se, December 2003.

[2] Boström, T., *A new generation of spectrally selective solar absorbers and thermal solar systems*. Licentiate's thesis from the department of Engineering Sciences at Uppsala University, Uppsala, 2004.

[3] Boström, T. *Design of a solar thermal system with high solar fraction in an extremely well insulated house*. in Proceedings of ISES. 2003. Göteborg, Sweden.

[4] Hastings, R. and M. Wall, eds. to be published. Sustainable solar housing, Volume 1. Strategies and solutions, Volume 2: Exemplary buildings and Technologies from IEA Task 28. James & James: London.

[5] Boström, T., W. Glad, C. Isaksson, F. Karlsson, M.-L. Persson, and A. Werner, 2003. *Tvärvetenskaplig analys av lågenergihusen i Lindås Park, Göteborg, Program Energisystem, arbetsnotat 25*.

[6] Osborn, D.E., 1993. *Selected Papers on Solar Radiation and Solar Thermal Systems*. Optical Engineering Press

[7] Kovacs, P. and U. Pettersson, SP Report 2002. Solar combi system, a comparison between vacuum tube and flat plate collectors using measurements and simulations, SP Swedish National Testing and Research Institute, Borås:20.

[8] Adsten, M., *Solar thermal collectors at high latitudes*. Ph.D. thesis from the department of Engineering Sciences at Uppsala University, Uppsala, 2002.

[9] Peres, B., 1995, *Optical modeling of solar collectors and booster reflectors under non stationary conditions*. Doctoral thesis from the department of Engineering Sciences at Uppsala University.

[10] Duffie, J.A. and W.A. Beckman, 1991. *Solar Engineering of Thermal Processes*. Wiley-Interscience, New York

[11] Peres, B. and C. Bales, 2002. A Solar Collector Model for TRNSYS Simulation and System Testing, SERC Dalarna University, Borlänge:

[12] Chant, V.G. and R. Håkansson, 1985. *The MINSUN simulation and optimisation program. Application and users guide.* IEA SH & C Task VII, Ottawa

[13] Fischer, S., W. Heidemann, H. Müller-Steinhagen, B. Perers, P. Bergquist, and B. Hellström. *Collector test method under quasi-dynamic conditions according to the European Standard EN 12975-2*. in Proceedings of ISES Solar World Congress. 2001. Adelaide, Australia.

[14] Kvist, H., 2003. Derob-LTH v1.0 for MS Windows, User's Manual, Department of Construction and Architecture, Lund Institute of Technology, Lund University, Lund, Sweden,

[15] Meteonorm 5.0 Global Meteorological Database for Solar Energy and Applied Meteorology, Meteotest, 2003.

[16] Dalenbäck, J.-O., 2002. Anneberg - Solar heating plant with seasonal storage in rock. CIT Energy Management AB, EU Project Report REB 0061/97,

[17] www.sp.se, March 2003.

[18] www.oeko.de/service/gemis/en/index.htm, February 2004.

[19] Karlsson, B. and G. Wilson. *MaReCo - A large asymmetric CPC for high latitudes*. in Proceedings of ISES Solar World Congress. 1999. Jerusalem, Israel.

[20] Granqvist, C.G., 1989. *Spectrally Selective Surfaces for Heating and Cooling Applications*. The International Society for Optical Engineering, Washington

[21] Agnihotri, O.P. and B.K. Gupta, 1981. *Solar Selective Surfaces*. John Wiley & Sons, New York

[22] Gordon, J., ed. 2001. Solar Energy, The State of the Art. James & James Ltd: London.

[23] Randich, E. and D.D. Allred, 1981, *Chemically vapor-deposited ZrB2 as a selective solar absorber*. Solar Energy Mater. **5**, p. 425.

[24] Orel, Z.C., 1999, *Characterisation of high-temperature-resistant spectrally selective paints for solar absorbers*. Solar Energy Mater. and Solar Cells. **57**, p. 291-301.

[25] Craighead, H.G. and R.A. Buhrman, 1977, *Optical properties of selectievely absorbing Ni/Al2O3 composite films*. Appl. Phys. L. **31**(7), p. 423-425.

[26] Andersson, Å., O. Hunderi, and C.G. Granqvist, 1980, *Nickel pigmented anodic aluminum oxide for selective absorption of solar energy*. J. Appl. Phys. **51**, p. 754-764.

[27] Sathiaraj, T. and R. Thangaraj, 1997, *The experimental and calculated optical properties of NI-Al2O3 coatings using effective medium theories*. J. Phys. D: Appl. Phys. **30**, p. 769-775.

[28] Simonis, F., M. van der Leij, and C.J. Hoogendoorn, 1979, *Physics of doped tin dioxide films for spectral selective surfaces*. Solar Energy Mater. **1**, p. 221.

[29] www.sunstrip.se, 2006.

[30] www.sunselect.de, 2006.

[31] Hoel, A., *Selective paint for thermal solar absorbers*. Master's thesis from the department of Engineering Sciences at Uppsala University, 1998, Q 98 010.

[32] www.mtisolar.com, 2006.

[33] www.tinox.de, 2006.

[34] Heavens, O.S., 1991. *Optical properties of thin solid films*. Dover Publications, New York

[35] Bruggeman, D.A.G., 1935, *Berechnung Verschiedener Physikalischer Konstanten von Heterogenen Substanzen*. Ann. Phys. **24**, p. 636-664.

[36] Meschede, D., 2002. *Gerthsen Physik*. 21 ed. Springer,

[37] Palik, E.D., 1985. *Handbook of Optical Constants of Solids*. Academic Press. Inc., Orlando

[38] Vicente, G., A. Morales, and M.T. Guiterrez, 2001, *Preparation and characterization of sol-gel TiO2 antireflective coatings for silicon*. Thin Solid Films. **391**, p. 133-137.

[39] Hu, L., T. Yoko, H. Kozuka, and S. Sakka, 1992, *Effects of solvent on properties of sol-gel-derived TiO2 coating films*. Thin Solid Films. **219**, p. 18-23.

[40] Wäckelgård, E., 1992, *A study of the optical properties of nickel pigmented anodized aluminum oxide on aluminum*. Proc. Soc. Photo-Opt. Istrum. Eng. **1727**, p. 82-86.

[41] Tadanaga, K., K. Iwashita, T. Minami, and N. Tohge, 1996, *Coating and Water Permeation Properties of SiO2 Thin Films Prepared by the Sol-Gel Method on Nylon-6 Substrates*. J. of Sol-Gel Sc. and Tech. **6**, p. 107-111.

[42] Dawnay, E.J.C., M.A. Fardad, M. Green, F. Horowitz, E.M. Yeatman, R.M. Almeida, H.C. Vasconcelos, M. Guglielmi, and A. Martucci, 1995, *Control and Characterisation of microsturcture in sol-gel films for optical device applications*. Adv. Mater. in Opt, p. 55-62.

[43] ed. Tesmer, J.R. and M. Nastasi, 1995. *Handbook of Modern Ion Beam Materials Analysis*. Material Research Society

[44] Assmann, W., H. Huber, C. Steinhausen, M. Dobler, H. Gliickler, and A. Weidinger, 1994, *Elastic recoil detection analysis with heavy ions*. Nucl. Instr. and Meth. **B89**, p. 131-139.

[45] Zhang, Y., H.J. Whitlow, T. Winzell, I.F. Bubb, T. Sajavaara, K. Arstila, and J. Keinonen, 1999, *Detection efficiency of time-of-flight energy elastic recoil detection analysis systems*. Nucl. Instr. and Meth. **B149**, p. 477-489.

[46] Lu, J., *Microstructure Aspects of Transition Metal Carbide Thin Films*. Inorganic Chemistry, 1998.

[47] Ward, L., 1998. *The optical constants of bulk materials and films*. J.W. Arrowsmith Ltd, Great Britain

[48] Theiss, M., 2002. *Hard and Software, CODE*. Aachen, Germany

[49] Shuxi, Z., C.-G. Ribbing, and E. Wäckelgård, 2004, *Optical constants of sputtered Ni/NiO solar absorber film - depth-profiled characterization*. Sol. Energy Mater. & Sol. Cells. **84**, p. 193-203.

[50] Boström, T., *Feasibility study of a solution-chemical method to produce spectrally selective surfaces for thermal solar absorbers*. Master's thesis from the department of Engineering Sciences at Uppsala University, Uppsala, 2002 (unpublished).

[51] Sakka, S., ed. 2005. Handbook of Sol-Gel Science and Technology. Vol. 1, Kluwer Academic Publishers: New York.

[52] Carlsson, B., U. Frei, M. Köhl, and K. Möller, SP Report 1994. Accelerated life testing of solar energy materials-Case study of some selective solar absorber coating materials for DHW Systems; A technical report of Task X solar materials research and development of the International Energy Agency Solar Heating and Cooling Program, Borås, Sweden:

[53] Wäckelgård, E., 1998, *A comparative study of the optical properties of nickel pigmented alumina films of different thicknesses exposed to elevated temperature and humidity*. Solar Energy Mater. and Solar Cells. **54**, p. 171-179.

[54] Carlsson, B., IEA SHC Task 27 draft report, 2004. Recommended qualification test procedure for solar absorber surface durability, Borås:

[55] Schade, M., 2006 (unpublished). Industrial adaptation of coating technique for absorber-surfaces in sun collectors, Uppsala:

Acta Universitatis Upsaliensis

Digital Comprehensive Summaries of Uppsala Dissertations from the Faculty of Science and Technology 225

Editor: The Dean of the Faculty of Science and Technology

A doctoral dissertation from the Faculty of Science and Technology, Uppsala University, is usually a summary of a number of papers. A few copies of the complete dissertation are kept at major Swedish research libraries, while the summary alone is distributed internationally through the series Digital Comprehensive Summaries of Uppsala Dissertations from the Faculty of Science and Technology. (Prior to January, 2005, the series was published under the title "Comprehensive Summaries of Uppsala Dissertations from the Faculty of Science and Technology".)

Distribution: publications.uu.se
urn:nbn:se:uu:diva-7160

ACTA
UNIVERSITATIS
UPSALIENSIS
UPPSALA
2006